CANADIAN THESES ON MICROFICHE

I.S.B.N.

THESES CANADIENNES SUR MICROFICHE

National Library of Canada
Collections Development Branch

Canadian Theses on
Microfiche Service

Ottawa, Canada
K1A 0N4

Bibliothèque nationale du Canada
Direction du développement des collections

Service des thèses canadiennes
sur microfiche

NOTICE

The quality of this microfiche is heavily dependent upon the quality of the original thesis submitted for microfilming. Every effort has been made to ensure the highest quality of reproduction possible.

If pages are missing, contact the university which granted the degree.

Some pages may have indistinct print especially if the original pages were typed with a poor typewriter ribbon or if the university sent us a poor photocopy.

Previously copyrighted materials (journal articles, published tests, etc.) are not filmed.

Reproduction in full or in part of this film is governed by the Canadian Copyright Act, R.S.C. 1970, c. C-30. Please read the authorization forms which accompany this thesis.

THIS DISSERTATION
HAS BEEN MICROFILMED
EXACTLY AS RECEIVED

AVIS

La qualité de cette microfiche dépend grandement de la qualité de la thèse soumise au microfilmage. Nous avons tout fait pour assurer une qualité supérieure de reproduction.

S'il manque des pages, veuillez communiquer avec l'université qui a conféré le grade.

La qualité d'impression de certaines pages peut laisser à désirer, surtout si les pages originales ont été dactylographiées à l'aide d'un ruban usé ou si l'université nous a fait parvenir une photocopie de mauvaise qualité.

Les documents qui font déjà l'objet d'un droit d'auteur (articles de revue, examens publiés, etc.) ne sont pas microfilmés.

La reproduction, même partielle, de ce microfilm est soumise à la Loi canadienne sur le droit d'auteur, SRC 1970, c. C-30. Veuillez prendre connaissance des formules d'autorisation qui accompagnent cette thèse.

LA THÈSE A ÉTÉ
MICROFILMÉE TELLE QUE
NOUS L'AVONS REÇUE

NL-339 (r. 82/08)

Canada

National Library of Canada | Bibliothèque nationale du Canada

Canadian Theses Division | Division des thèses canadiennes

Ottawa, Canada
K1A 0N4

0-315-06107-3

54027

PERMISSION TO MICROFILM — AUTORISATION DE MICROFILMER

• Please print or type — Écrire en lettres moulées ou dactylographier

Full Name of Author — Nom complet de l'auteur

Ronald Philip Schmidt

Date of Birth — Date de naissance	Country of Birth — Lieu de naissance
July 12, 1950	Canada

Permanent Address — Résidence fixe

10330 - 144 St
Edmonton, Alta.
T5N 2V2

Title of Thesis — Titre de la thèse

The Comparative Sensitivity of Bone Scintigraphy and Radiography in the Early Detection of Experimental Osteomyelitis

University — Université

University of Alberta

Degree for which thesis was presented — Grade pour lequel cette thèse fut présentée

M. Sc. in Radiopharmacy

Year this degree conferred — Année d'obtention de ce grade	Name of Supervisor — Nom du directeur de thèse
1981	Dr. A. Shysh

Permission is hereby granted to the NATIONAL LIBRARY OF CANADA to microfilm this thesis and to lend or sell copies of the film.

The author reserves other publication rights, and neither the thesis nor extensive extracts from it may be printed or otherwise reproduced without the author's written permission.

L'autorisation est, par la présente, accordée à la BIBLIOTHÈQUE NATIONALE DU CANADA de microfilmer cette thèse et de prêter ou de vendre des exemplaires du film.

L'auteur se réserve les autres droits de publication; ni la thèse ni de longs extraits de celle-ci ne doivent être imprimés ou autrement reproduits sans l'autorisation écrite de l'auteur.

Date	Signature
October 8, 1981.	Ronald Philip Schmidt

NL-91 (4/77)

THE UNIVERSITY OF ALBERTA

THE COMPARATIVE SENSITIVITY OF BONE SCINTIGRAPHY AND RADIOGRAPHY IN THE EARLY DETECTION OF EXPERIMENTAL OSTEOMYELITIS

by

© RONALD PHILIP SCHMIDT

A THESIS

SUBMITTED TO THE FACULTY OF GRADUATE STUDIES AND RESEARCH

IN PARTIAL FULFILMENT OF THE REQUIREMENTS FOR THE DEGREE

OF MASTER OF SCIENCE

IN

RADIOPHARMACY

FACULTY OF PHARMACY AND PHARMACEUTICAL SCIENCES

EDMONTON, ALBERTA

FALL, 1981

THE UNIVERSITY OF ALBERTA

RELEASE FORM

NAME OF AUTHOR - RONALD PHILIP SCHMIDT

TITLE OF THESIS - THE COMPARATIVE SENSITIVITY OF BONE SCINTIGRAPHY AND RADIOGRAPHY IN THE EARLY DETECTION OF EXPERIMENTAL OSTEOMYELITIS

DEGREE FOR WHICH THESIS WAS PRESENTED - Master of Science

YEAR THIS DEGREE GRANTED - 1981

Permission is hereby granted to THE UNIVERSITY OF ALBERTA LIBRARY to reproduce single copies of this thesis and to lend or sell such copies for private, scholarly or scientific research purposes only.

The author reserves other publication rights, and neither the thesis nor extensive extracts from it may be printed or otherwise reproduced without the author's written permission.

(Signed) Ronald Philip Schmidt

PERMANENT ADDRESS:
Ronald Philip Schmidt
10330 - 144 Street
Edmonton, Alberta
T5N 2V2

DATED October 2 19 81.

THE UNIVERSITY OF ALBERTA

FACULTY OF GRADUATE STUDIES AND RESEARCH

The undersigned certify that they have read, and recommend to the Faculty of Graduate Studies and Research, for acceptance, a thesis entitled "The Comparative Sensitivity of Bone Scintigraphy and Radiography in the Early Detection of Experimental Osteomyelitis" submitted by Ronald Philip Schmidt in partial fulfilment of the requirements for the degree of Master of Science in Radiopharmacy.

.....
Supervisor

.....

.....

.....
External Examiner

Date October 7, 1981.....

Dedicated to Lynda

ABSTRACT

Several procedures for the induction of osteomyelitis in a rabbit model were evaluated. The animal model which best seemed to simulate the human disease was studied by radiological and scintigraphic methods in an effort to assess the relative efficiency of these modalities for the early detection of the disease state.

Diagnostic radiology demonstrated a sensitivity of 0.89 and a specificity of 0.68 for detecting osteomyelitis in this animal model while scintigraphic analysis provided a sensitivity of 0.42 and a specificity of 0.95. Scintigraphic detection of the experimentally induced infection site was often hampered by the normal high uptake of radiotracer in the growing epiphyseal regions in the young rabbit. Interobserver variability was higher in the interpretation of the radiographs than in the reading of the scintiscans. Increased uptake of Tc-99m methylene diphosphonate (MDP) in the affected bone relative to the contralateral normal bone was seen within ten minutes of intravenous injection. Static uptake studies also consistently showed more uptake of Tc-99m MDP by affected bone than contralateral normal bone.

Other scintigraphic studies in this animal model, employing ^{18}F-sodium fluoride, ^{67}Ga citrate, ^{99m}Tc sulphur colloid bone marrow uptake, and ^{99m}Tc sulphur colloid leukocyte scintiscans have shown patterns of uptake consistent with the development and progression of osteomyelitis.

ACKNOWLEDGEMENTS

I would like to express my sincere gratitude to Dr. A. Shysh for his encouragement and guidance throughout this project.

I would also like to say a special thank you to Dr. F.I. Jackson, Dr. B.C. Lentle, Dr. W. Castor, Dr. H. Ferri, and Dr. R. Ludwig for their help with this work.

The work of Dr. G.R. Johnson and Dr. R.J. Lewis in performing the histopathological examinations is appreciated.

Thanks also to the Edmonton Radiopharmacy Centre for providing materials and, in particular, Mr. J.R. Scott for his aid throughout this project.

The help of Mr. C. Ediss and Mr. S. McQuarrie is appreciated.

Dr. H.R. Hooper's assistance with the statistical analysis was most helpful.

Thanks also to Dr. L.I. Wiebe and Mr. J. Mercer for providing the F-18 sodium fluoride for this work.

Ms. Jean Brooks' preparation of the figures for this manuscript and the photographic skills of Mr. Frank Locicero are appreciated.

Special thanks to Ms. J. Roseboom for the hours spent typing and proofreading this manuscript.

Financial aid in the form of a graduate teaching assistantship is gratefully acknowledged.

TABLE OF CONTENTS

	Page
ABSTRACT	v
ACKNOWLEDGEMENTS	vi
TABLE OF CONTENTS	vii
LIST OF TABLES	x
LIST OF FIGURES	xi
LIST OF PHOTOGRAPHIC PLATES	xii
I. INTRODUCTION	1
II. SURVEY OF THE LITERATURE	4
A. Osteomyelitis	5
B. Animal Models for Osteomyelitis	9
C. Radiographic Detection of Osteomyelitis	12
D. Bone Scintiscanning	13
E. ^{99m}Tc-Phosphates	14
F. Skeletal Metabolism	18
G. Studies Relating Radiographs and Bone Scintiscans for Detection of Osteomyelitis	22
H. Dynamic Uptake in Bone	25
I. ^{67}Ga Citrate and Inflammatory Lesions	26
J. ^{18}F-Fluoride Uptake by Bone	28
K. Bone Marrow Scintiscanning	30
L. ^{99m}Tc-Sulphur Colloid Labelled Granulocytes	32
III. MATERIALS AND METHODS	33
A. Experimental Animals	34
B. Microorganisms	34

		Page
C.	Radiopharmaceuticals and Reagents	35
	1. ^{99m}Tc Pyrophosphate	35
	2. ^{99m}Tc Methylene Diphosphonate	35
	3. Macroaggregated Human Serum Albumin	36
	4. ^{99m}Tc-Labelled White Blood Cells	38
	5. Gallium-67 Citrate Distribution Study	38
	6. ^{18}Fluorine	39
D.	Radiology	40
E.	Bone Scans	41
F.	Investigational Procedures	41
	1. Dynamic Uptake Studies	41
	2. Radio-activity Uptake Studies	42
V.	RESULTS AND DISCUSSION	44
A.	Development of an Osteomyelitis Model	45
	1. Rabbit Model for Osteomyelitis	45
	2. Controls	47
	3. Osteomyelitis Model Using Bacterially Impregnated Macroaggregated Human Serum Albumin	48
	4. Cat Model for Osteomyelitis	52
	5. Alternate Rabbit Model for Osteomyelitis	52
B.	Histopathological Examinations	53
C.	Comparison of Scintigraphic and Radiographic Methods for Detection of Osteomyelitis	55
D.	Analysis of Radiographic and Scintigraphic Data	76
	1. Analysis of Data from Experiments 1 and 2	76
	2. Analysis of Data from Experiments 3, 4, and 5	80

Page

E. Dynamic Uptake of Tc-99m MDP in Normal and Infected Rabbit Limbs 90

F. Static Uptake Studies of ^{99m}Tc Methylene Diphosphonate 93

G. Further Diagnostic Scintigraphic Evaluations of this Rabbit Model for Osteomyelitis 103

1. ^{67}Ga Citrate Scintigram and Tissue Distribution Study 104

2. 18F-Fluoride Uptake Study 108

3. ^{99m}Tc Sulphur Colloid Labelled Granulocytes .. 111

4. Bone Marrow Uptake of ^{99m}Tc Sulphur Colloid .. 114

V. SUMMARY AND CONCLUSIONS 118

VI. BIBLIOGRAPHY 121

VII. PUBLICATIONS 138

LIST OF TABLES

Table	Description	Page
1	Comparison of ^{99m}Tc Bone-Seeking Radiopharmaceuticals in Rabbits	16
2	Radiation Absorbed Dose Estimates in Humans	23
3	Osteomyelitis Positive Rabbits	50
4	Data Reduction of Experiment 1	77
5	Data Reduction of Experiment 2	78
6	Data Reduction of Experiment 3	81
7	Data Reduction of Experiment 4	82
8	Data Reduction of Experiment 5	83
9	Summary of Radiographs and Scintigraphic Evaluations	84
10	Final Data Reduction of Experiments 3, 4 and 5	87
11	Static Uptake Study Results of Rabbit #1	96
12	Static Uptake Study Results of Rabbit #2	97
13	Static Uptake Study Results of Rabbit #3	98
14	Static Uptake Study Results of Rabbit #4	99
15	Static Uptake Study Results of Rabbit #6	100
16	Static Uptake Study Results of Rabbit #7	101
17	Static Uptake Study Results of Rabbit #8	102
18	Tissue Concentration of ^{67}Ga Citrate in an Osteomyelitis-Positive Rabbit	109

LIST OF FIGURES

Figure	Description	Page
I	Summary of evaluations of bone scintiscans and radiographs of experiment No. 1	58
II	Summary of evaluations of bone scintiscans and radiographs of experiment No. 2	60
III	Summary of evaluations of bone scintiscans and radiographs of experiment No. 3	67
IV	Summary of evaluations of bone scintiscans and radiographs of experiment No. 4	69
V	Summary of evaluations of bone scintiscens and radiographs of experiment No. 5	74
VI	Dynamic Uptake of ^{99m}Tc Methylene Diphosphonate in a Normal Rabbit	92
VII	Dynamic Uptake of ^{99m}Tc Methylene Diphosphonate in an Osteomyelitis-Positive Rabbit	92

LIST OF PHOTOGRAPHIC PLATES

Plate	Description	Page
1	Radiograph of hind limbs of a rabbit with hematogenous osteomyelitis	61
2	Scintigram (Tc-99m-MDP) of hind limbs of a rabbit with hematogenous osteomyelitis	62
3	Radiograph of hind limbs of a rabbit displaying gross osteomyelitic lesions	63
4	Scintigram (Tc-99m-MDP) of hind limbs of a rabbit with advanced osteomyelitic lesions	64
5	Radiograph of hind limbs of a rabbit displaying gross osteomyelitic lesions	105
6	Scintigram (Tc-99m-MDP) of hind limbs of a rabbit displaying gross osteomyelitic lesions	106
7	Scintigraphic (Ga-67-citrate) of hind limbs of a rabbit with advanced osteomyelitic lesions	107
8	Scintigram (F-18-fluoride) of hind limbs of a rabbit with osteomyelitic lesions	110
9	Radiograph of hind limb of a rabbit with osteomyelitic lesions	112
10	Scintigram (Tc-99m-MDP) of hind limbs of a rabbit with osteomyelitic lesions	113
11	Scintigram (Tc-99m-sulphur colloid) of hind limbs of a rabbit with osteomyelitic lesions 26 days after inoculation	115
12	Scintigram (Tc-99m-sulphur colloid) of hind limbs of a rabbit 36 days after inoculation	116

I. INTRODUCTION

Osteomyelitis is an insidious bone infection difficult to diagnose clinically in its early stages because of its inherent characteristics. Signs and symptoms include a positive blood culture, elevated temperature, edema, pain, joint tenderness, soft tissue swelling, erythema, limping, and disuse of the affected part.

Early diagnosis is essential to ensure the likelihood of complete recovery and to prevent the possible crippling effects of the disease by administering prompt, effective antibiotic therapy. Currently, therapy is individually modified to each patient and may be up to six weeks in duration.

Historically, diagnosis was performed either by observing roentgenographic changes over a period of time or by noting gross bone structural malformation - specifically destructive bone changes and periosteal new bone formation as well as soft tissue inflammation. However, there is a latent period, usually seven to fourteen days between the initial onset of the clinically recognized signs and symptoms and sufficient radiologically visible bone changes to make the diagnosis.

Recently, a new diagnostic technique has gained clinical favor - the use of radioactive bone scanning agents to make an early diagnosis on a functional or physiological level.

Current literature indicates that suspected cases of osteomyelitis have been confirmed with the use of bone-seeking radioagents within 48 hours of the onset of appropriate signs and symptoms.

The purpose of this research project was to compare the relative sensitivities of current diagnostic radiological techniques with

presently used bone-seeking radiopharmaceuticals in the early diagnosis of osteomyelitis.

To accomplish this, a simulation of the disease state was induced in male New Zealand white rabbits. Parallel series of bone scans and radiographs were made of each animal during the course of the disease and studies were conducted to compare the relative sensitivities of these two approaches for the early detection of osteomyelitis.

II. SURVEY OF THE LITERATURE

A. OSTEOMYELITIS

Osteomyelitis is a bone infection which is most prevalent in the pediatric age group and occurs most frequently in the long bones, especially the tibia and femur. These diseases may localize or may diffuse to affect periosteum, cortex, cancellous tissue, or marrow. Osteomyelitis may be acute or chronic. Waldvogel (Wa70) classifies osteomyelitis into three categories: hematogenous osteomyelitis, osteomyelitis resulting from contiguous infection foci, and osteomyelitis accompanying peripheral vascular disorders.

While a complete discussion of bone physiology is beyond the scope of this thesis the following section reviews some pertinent aspects of bone structure as related to processes of bone infection (Ga69, Wa70, Wa70a, Wa70b).

Long bones consist of a shaft or diaphysis and two ends known as the epiphyses which are usually wider than the diaphysis. Completely cartilaginous epiphyses are found on growing bones but if ossification of the epiphysis has begun, cartilaginous discs separate the epiphysis from the diaphysis. The metaphysis is the wider part of the diaphysis contiguous with the epiphyseal disc and also contains the growth zone of the bone. The mature long bone metaphysis and epiphysis are continuous.

A tube of compact or cortical bone makes up the long bone shaft. The cavity in the shaft is the medullary or marrow cavity and contains either red or yellow marrow or both in combination. The metaphysis and epiphysis are composed of trabeculae, irregular anastomosing bars, forming cancellous or spongy bone. Marrow occupies the spaces between

the trabeculae. Compact bone makes up the external surfaces of the metaphysis and epiphysis, all of which are ultimately covered by a cartilage.

Periosteum, a connective tissue which covers all living bones, is composed of two layers - a fibrous outer, limiting membrane containing blood vessels and an inner layer which is relatively less dense and looser, containing a network of elastic fibres. Another tissue, the endosteum, lines the medullary cavity.

The periosteum is contiguous with the joint capsule although it is not associated with the joint cartilage. Tendons and muscles are attached to the periosteum.

The blood vessels enter the bone through many foramina or openings in the bone. Most of the foramina are located close to the articular surface edges. The veins usually leave the bones via the largest foramina. The foramina on the shaft are generally smaller except for one or two large nutrient foramina which form obliquely slanting canals containing the nutrient vessels feeding the bone marrow. Bone tissue is metabollically active. Rapid synthesis and resorption of bone tissue require a sufficient vascular supply. Acute hematogenous osteomyelitis typically affects long bone metaphyses.

Waldvogel (Wa70) reports in a general review article that rabbits are susceptible to osteomyelitis because the blood vessels proximal to the metaphyseal aspect of the growth plate present an available site for bacterial infection. The nutrient capillaries approaching the epiphyseal growth plate make sharp loops and join large sinusoid veins in the marrow cavity producing a suddenly sluggish blood flow. Three reasons are suggested for the observed usual localization of infection

in the metaphysis (ibid). First, an ascending or afferent capillary loop usually is a single structure and has a diameter of 8 μm while the descending loops are usually multiple and their diameters range from 15 to 60 μm to produce a slower, more turbulent blood flow (ibid). Secondly, phagocytic lining cells are absent in the afferent loop, and while the efferent loop has such cells, they are functionally inactive (ibid). Thirdly, because the capillary loops remain single structures and do not communicate with any other structures, any occlusion by bacteria or microthrombi would result in an avascular necrosis (ibid). If bacteria establish themselves in a suitable locus, a series of physical changes soon occur in the area of infection (ibid). The host responds with immune and inflammatory responses in an attempt to isolate and annihilate the microorganisms. The infected bone responds with an acute inflammatory response and exudes a fluid containing polymorphonuclear leukocytes and fibrin. Within the bone vascular ischaemia, bacterial products, and enzymes liberated from dying polymorphonuclear leukocytes will possibly damage and may even kill marrow and perhaps trabecular bone. If, at this stage, the bacteria are killed, the bone will usually heal and be restored to its normal state. If, however, the disease state progresses beyond this point, the pathophysiologic situation of the bone changes radically and the overall status of the bone deteriorates (ibid). The case of an infection in bone is different from most other body infections in that a situation exists where a small volume of soft tissue is completely encapsulated by a hard outer casing. As the bone produces more exudate, the internal pressure of the bone increases and the exudate forces its way through the medullary cavity

and into the Volkmans and Haversian canals, which are the canals of the bone cortex. What happens next is dependent on two factors - firstly the thickness of the cortex and secondly the thickness and degree of periosteum attachment to the cortex.

In the pediatric situation, the metaphyseal cortex is typically thin and has associated with it a loosely attached periosteum (ibid). An infection within the metaphysis can push its exudate through the cortex and elevate the periosteum resulting in a interruption of the blood supply to the cortical bone (ibid). This ends in the death of the outer half of the afflicted cortex. As the bone dies, sequestra form. Sequestra are bits of dead bone which separate from unaffected bone during the process of necrosis. Pus eventually surrounds the sequestra. Repair is composed essentially of fibrous tissue production and new bone formation in the medullary canal. Involucrum, new bone formed under the periosteum when the periosteum is lifted, can also be observed. In such infections in the pediatric age group much involucrum tissue can be seen and can surround the necrotic cortex. Because the sequestra are isolated from a blood supply a unique set of circumstances are set up (ibid): (1) the repair processes are slowed considerably, (2) the pathogenic bacteria which could reinfect the bone are isolated, and (3) the rate at which antibodies and antibiotics reach the bacteria are slowed.

In infants the diaphysis is usually involved initially and the infection spreads rapidly to the epiphysis and joint spaces. Since the metaphyseal cortex is thin and immature, the exudate typically lifts and perforates the periosteum to affect periosteal tissue often with remarkable bone destruction and involucrum formation.

The adult situation is different in that the cortex is thicker and possess a much more rigidly bound periosteum (ibid). Any internal infection here tends to remain within the intramedullary cavity and can potentially spread along the canal and through the articular cartilage to the joint space. Usually the cancellous bone is destroyed, cortical bone disappears from the endosteal side, and some new bone formation occurs (ibid). Soft tissue abscesses can be seen if pus permeates the cortex and periosteum to reach soft tissue. Since the periosteum is not lifted off the bone, the blood supply remains intact and sequestra are rarely seen (ibid).

B. ANIMAL MODELS FOR OSTEOMYELITIS

A number of various procedures for the induction of osteomyelitis in animal models have been reported in the literature. The following section reviews some of the documented experimental methods that are relevant to this thesis.

In 1884 Rodet (Ro73) reported an animal model for osteomyelitis produced by intravenous injection of a yellow orange microbe grown in chicken bouillon. Starr (St22) presented a dog model for osteomyelitis produced by injection of disease-causing microorganisms into a nutrient artery or physically damaged metaphysis. However, all animals died within two days of injection so that no later developing symptoms of the disease could be observed. Starr stated (p. 557) "we found great difficulty in producing osteomyelitis in the dog, even with staphylococci or streptococci of known virulence in man". Haldeman (Ha34) presented a rabbit model produced by insertion of S. aureus into a hole drilled in the upper end of the tibia. Thompson and Dubos (Th38)

announced a rabbit model produced by intravenous injection of S. aureus. Wilensky (Wi27) questioned unsuccessful animal models and emphasized the importance of establishing the necessary milieu for embolus-thrombus formation. Scheman et al. (Sc41) attempted to reproduce published animal models but were unable to duplicate the progressive bone lesion characteristic of the disease and instead found that the animals died with abscesses in the liver, kidney or spleen with only infrequent bone involvement. This group reported that the necessary aseptic necrosis of bone can be induced by the presence of sodium morrhuate which can subsequently develop into osteomyelitis given the presence of Staphylococcus aureus.

More animal models for osteomyelitis have recently been reported in the literature. Deysine et al. (De76) reported on a canine model induced by injecting a preparation of barium sulfate and S. aureus into the nutrient artery of the tibia. Nickerson et al. (Ni69) presented a model induced by the injection of a mixture of S. aureus and lanolin into the medullary cavity of the rabbit femur. Norden (No70) reported a protocol for a rabbit model for osteomyelitis. After shaving the right hind limb and cleaning the injection site with alcohol an 18-gauge needle was inserted through the skin and lateral aspect of the metaphysis into the medullary compartment of the tibia. Small volumes (0.1 ml) of sodium morrhuate, S. aureus suspension, and sterile saline were then passaged through the needle into the medullary cavity. Although the strain of S. aureus employed was isolated from a child with osteomyelitis, Norden reported that the use of only the bacteria or sclerosing agent alone produced no evidence of the disease process, and furthermore bone cultures taken 14 and 16 days post-inoculation were

always sterile. Both S. aureus and sodium morrhuate were needed to cause osteomyelitis. Norden further stated that this model was similar to the human condition in that: "(1) the animals favored the infected limb, (2) the animals showed evidence of systemic infection with elevated sedimentation rate and leukocyte count, and loss of weight, (3) the affected leg appeared swollen and warm as early as 7 days after injection, (4) radiographic changes of osteomyelitis were not seen until 14-21 days after infection. Radiologic changes consisted of destruction of the shaft of the tibia, elevation and disruption of the periosteum, new bone deposition, and sequestrum formation". Norden, however, used no control animals in his experiments. Rinsky et al. (Ri77) also used Norden's model but prepared controls by injecting sterile culture medium instead of bacteria. Rafkin et al. (Ra74) reported a rabbit model induced by injecting a mixture of 0.1 ml sodium morrhuate and 1 ml S. aureus suspension into the tibial medullary cavity and then sealing the hole with bone wax to prevent subcutaneous infections. Controls were provided by injecting normal saline into the contralateral tibia. Deysine et al. (De75) reported a similar procedure in which the rabbits' periosteum was stripped for 3 mm, a 1 mm burr was used to puncture the bone, and a needle forced into the medulla. Sterile normal saline was injected into the left tibia and a mixture of S. aureus and sodium morrhuate into the contralateral bone. The holes were then sealed with sterile bone wax. Norris et al. (No81) reported a rabbit model which involves an antigenic stimulus but no viable microorganisms. This involved culturing S. aureus procurred from a patient with acute osteomyelitis, followed by suspension in distilled water, and finally a

heat-killing process. The final suspension was injected together with sodium morrhuate into the medullary cavity of the tibia.

C. RADIOGRAPHIC DETECTION OF OSTEOMYELITIS

Independent reports by Capitanio and Kirkpatrick (Ca70) and by Treves et al. (Tr76) indicate that in acute cases of osteomyelitis, roentgenograms have demonstrated visible soft tissue changes within seventy-two hours of the onset of symptoms. Furthermore, their work suggests that three different types of changes may be observed. These include the following: firstly, a local, deep swelling of the soft tissue proximal to the metaphysis with contiguous shifting of fat lines but without superficial edema, secondly, a larger volume of tissue involvement accompanied by destruction of the lucent intramuscle planes, and thirdly, subcutaneous edema. These authors stressed that such changes are small and are unlikely to be recognized unless symmetrical roentgenograms of both extremities are made at the same time for comparison. Moreover, other reports show that for bone changes to be seen radiographically, 30% to 50% of the mineral must be removed from the bone matrix (Ba48, Sn57). Such regions of bone involvement are often poorly defined and irregular in nature. If the lesion is not extensive or if it is deep in the bone, the formation of new bone under the periosteum may be the earliest or possibly even the only sign of osteomyelitis (Ae68). If the infection is deep within the bone, it may be hidden by superimposed structures such as sclerotic bone normally found surrounding the inflammatory bones when the process of healing is initiated (Ae68). The classic radiograms characterized by sclerosis and

irregular thickening of the bone to produce abnormal bone architecture are not seen until 10-12 days after the onset of symptoms (Ca70).

D. BONE SCINTISCANNING

Bone scintiscanning is one of the most commonly used diagnostic procedures employed in nuclear medicine today. Perhaps, in its simplest sense, bone scintiscanning procedures can be viewed as functional examinations of the skeletal system. Bone scintigraphic imaging procedures have been adopted for many clinical investigations such as the detection of occult fractures not seen on radiographs, evaluation of chemotherapy, and assessment of arthritis involvement. A complete review of such procedures is beyond the scope of this discussion but extensive information is readily available in many textbooks of nuclear medicine. For the purpose of this thesis, the literature review will be confined to bone scintigraphy as related to detection of osteomyelitis.

Bauer and Wendeberg (Ba59) reported data from two patients who presented with ostemyelitis and who were injected intravenously with strontium-85. Count rates obtained over both the affected and contralateral unaffected bones demonstrated increased levels of radioactivity over the infected bone relative to the normal bone. One of these two cases showed increased uptake of radiotracer before any lesion was evident in the radiograph.

Some radioisotopes used for bone scintigraphy include ^{47}Ca, ^{85}Sr, ^{87m}Sr, ^{18}F, and ^{99m}Tc.

^{47}Ca possesses, perhaps, the most physiologic properties of these radionuclides but is considered unsuitable for clinical use because of

its associated β^- - decay, high γ-energy (1.31 MeV), and long physical half-life (4.5 days) (Wa68).

The radioisotopes of strontium are handled by the body as anionic substitutes for calcium and generally are metabolized in a similar fashion as calcium but not identically (Ba58). The major drawback to the use of this element is long plasma retention and slow excretion which necessitates delaying the scan as long as possible to get suitable clinical information (Fl61).

E. ^{99m}Tc-PHOSPHATES

At the present time, the most widely used bone scanning agents are various Tc-99m labelled phosphate complexes. These complexes are usually labelled by a stannous ion reduction procedure of sodium pertechnetate obtained from commercially available radionuclide generators (Su71, Su72, St74). The original polyphosphate compound has been modified over the past decade to produce many analogues including pyrophosphate (PPI), imidodiphosphate (IDP), diphosphonate (EHDP), and others (Da76, Su76, Su75). Davis and Jones (Da76) reported data on the biodistribution of the following ^{99m}Tc-labelled phosphate and phosphonate agents in rabbits expressed as per cent of total activity injected two hours after administration: imidodiphosphate (also called IDP), methylene diphosphonate (also called MDP), 1-aminoethylidene diphosphonate (also called AEDP), 1-hydroxyethylidene-1, 1-diphosphonic acid (also called EHDP), pyrophosphate (also called PPi), ethylenediamine tetra (methylene phosphonic acid (also called EDTMP), triethylenedramine tetra (methylene phosphonic acid) (also called TENTMP), and diethylenetriamine penta (methylene phosphonic acid) (also

called DTPMP) as in Table 1. Subramanian et al. (Su76) state that the stability of these compounds varies only slightly. Because methylene diphosphonate has the most rapid blood clearance and most quickly establishes a high lesion-to-background ratio (Da76), it has gained wide-spread use as a bone-seeking radiopharamaceutical.

An overview of factors involved in uptake of ^{99m}Tc-phosphate complexes by bone was presented by Frances et al. (Fr79) in which the following points were made: (1) These radiopharmaceuticals are very stable and variations in labelling and injection procedure have very little effect on stability although one report by Henkin et al. (He81) reported that a study of incubation times for ^{99m}Tc-MDP ranging from 30 to 121 minutes indicated that longer incubation periods produced better scintiscans. (2) Two major factors involved in skeletal uptake of phosphates and phosphonates are vascularity and skeletal metabolism. Francis et al. (Fr79) also reported that other important factors are: "the composition and surface area of the specific calcium phosphate present in bone where the Tc-99m ligand can diffuse: the solubility of the calcium ligand salt formed on the surface of the calcium phosphate in bone; the strength of the Tc-99m ligand complex which determines its stability while circulating ... to the bone and the structure of the ligand with which the reduced technetium species reacts to form a stable complex. Additional factors such as size of the technetium-99m complex, its charge and protein binding potential can also have an effect on its diffusion from the vascular system and its reactivity with bone".

The vascular system delivers the radiopharmaceutical to the bone. Wootton (Wo74) and Garnett et al. (Ga75) stated that ^{99m}Tc-pyrophosphate demonstrates an extraction ratio of 64% compared to fluorine-18 which is

TABLE 1

Comparison of ^{99m}Tc Bone Seeking Radiopharmaceuticals in Rabbits*

(Davis, MA and Jones, AG: Comparison of ^{99m}Tc-Labeled phosphate and phosphonate agents for skeletal imaging. Seminars in Nuclear Medicine 6: 19-31, 1976)

ORGAN	IDP	MDP	HEDP	AEDP	PPi	ENTMP	TENTMP	DTPMP
Blood	2.9	1.0	1.4	1.3	3.8	6.3	3.6	3.7
Urine	47.4	39.5	42.1	50.7	36.4	43.2	63.4	60.9
Total Skeleton	70.6	61.2	66.2	58.1	38.4	35.3	25.0	28.1
Bone: Blood Ratio	24.2	63.8	46.6	43.4	10.2	5.6	7.0	7.6

* Percent of injected dose, two hours after intravenous injection

considered to be 100% extracted. Lavender et al. (La79) reported work showing that a change in blood flow rate of 100% in a canine tibial artery produced a change in diphosphonate uptake of 800% and concluded that changes in blood flow rates can produce dramatic changes in bone uptake of radiotracer but that other factors are also involved. Hughes et al. (Hu78) reported a four compartment blood clearance curve for ^{99m}Tc-MDP while Makler and Charkes (Ma80) published results on a five compartment model for ^{99m}Tc-MDP in which they reported that less ^{99m}Tc-MDP than ^{18}F is extracted by bone (43% vs. 60%) than that reported by other investigators. Furthermore, they also hypothesized that a slower rate of diffusion into a smaller distribution space (extracellular fluid) was the prime factor to explain lower bone uptake of ^{99m}Tc-MDP compared to ^{18}F (Ma80). Moreover, these authors stated that optimum scintiscans could be obtained 4-6 hours after intravenous injection and should be taken for a fixed total number of counts rather than for a fixed time. This model of uptake of ^{99m}Tc-MDP also showed little increase in uptake of radiotracer when vascular flow increased significantly (Ma80).

Subramanian et al. (Su75) interpreted the slower blood clearance associated with ^{99m}Tc-pyrophosphate versus ^{99m}Tc-MDP as the result of a larger fraction of the labelled pyrophosphate complex being protein bound so that bone uptake and urinary excretion were delayed. Saha and Boyd (Sa78) suggested that release of the radiolabelled pyrophosphate from the plasma proteins is slower than the rate of bone uptake and urinary excretion of free ^{99m}Tc-pyrophosphate. They also reported that lower molecular weight plasma proteins released the radiotracer at slower rates than the higher molecular weight plasma proteins. Later

work by Saha and Boyd (Sa79) suggested that plasma clearance of protein bound ^{99m}Tc-methylene diphosphonate is much slower than the rate of uptake by bone and urinary excretion. Krishnamurthy et al. (Kr74) reported that the alpha- and beta-globulins are primarily associated with plasma binding of ^{99m}Tc-polyphosphates and pyrophosphate.

F. SKELETAL METABOLISM

Guillemart et al. (Gu80) found that at thirty minutes after intravenous administration of technetium-stannous pyrophosphate and ^{45}Ca, localization of both radiotracers reflected the vascular distribution in bone and calcified cartilage but that the technetium radioactivity was basically distributed to bone although not tightly bound. However, autoradiographic patterns were constant in the diaphysis throughout the experiment which the authors interpreted as local retention of the radiotracer so that they regarded the phosphate molecule as a "surface-seeker" rather than a "volume-seeker" such as ^{45}Ca which distributes throughout the bone tissue.

Kaye et al. (Ka75) postulated that ^{99m}Tc - bone-seeking radiopharmaceuticals are deposited to some extent on the organic matrix of bone in such disease states as osteomalacia but Francis et al. (Fr79) suggested that localization probably occurs as the process of the ^{99m}Tc-ligand complex reacting with the nuclei of calcium phosphate in the uncalcified bone matrix and not because of specific absorption or interaction with the organic matrix of the skeleton. They postulate that the rate of incorporation of calcium phosphate in the bone and maturity of the bone influence the type of inorganic calcium phosphate found in bone. Mature bone is composed of cell crystallized

hydroxyapatite [$Ca_{10}(OH)_2(PO_4)6$)] which is found as needlelike crystallites 200-600 Å in length and 25-75 Å in diameter or as plates 400 Å long and wide and about 50 Å thick (Fr79)." The molar Ca/P ratio of these mature crystals is close to the theoretical 1.67 for hydroxyapatite. If, however, bone is examined in an area of rapid metabolic formation such as in embryonic bone, newly forming bone or in lesions such as Paget's disease, the calcium phosphate present is of low density and high hydration, is amorphorous (by x-ray or electron microscopy), and can have a molar Ca/P as low as 1.4 (p. 607)" (Fr79). The authors feel that mixtures of calcium phosphates of different hydration states such as $CaHPO_4$, $Ca_4H(PO_4)_3$, and $Ca_3(PO_4)_2$ are found in areas of rapid metabolic formation. The exact kinetics of reactions between the radiopharmaceutical and these various phases is not known but it is accepted that the amount of absorption is directly proportional to available surface area. Francis et al. (Fr.68) reported that stannous tin, indium, and gallium react directly with the phosphate anion of bone to produce an insoluble phosphate tightly bound to the inorganic phase. Anions such as diphosphonate, pyrophosphate, polyphosphate, and fluoride react directly with calcium hydroxyapatite to produce thin layers of insoluble calcium salts also strongly bound to the inorganic phase of bone (Fr79). These workers state that important factors for ligand superiority are stability of the radiolabelled agent, solubility of the phosphonate, presence of the hydroxygroup, and solubility of the phosphonate calcium salt which apply also to areas of osteogenesis where the face of the hydroxyapatite surface is elevated relative to the other apatite faces and also because the early nonopatite states of calcium phosphonate exist.

The mechanism of incorporation of ^{99m}Tc bone-seeking radiopharmaceuticals at the intracellular fluid-bone interface is not completely known. Jones et al. (Jo76) suggested that the ^{99m}Tc-phosphorous compound is carried as an intact unit to the bone where it dissociates because of the affinity of the phosphorous moiety for the calcium phosphate of the bone whereupon the ^{99m}Tc is stored in the bone as the hydrolyzed oxide. Francis et al. (Fr79) presented evidence that tin is not necessary for ^{99m}Tc-phosphorous compounds to localize in bone. Tofe and Francis (To74) reported data showing that the ratio of technetium to diphosphonate in bone does not vary between 3 and 24 hours after administration, indicating that the complex is transported to the bone and stays there as a unit. Rosenthall and Kaye (Ro76) reported a series of experiments using rachitic and lathyritic rats examining the pharmacology of the phosphate complexes, especially pyrophosphate in which they concluded that ^{99m}Tc changed the kinetics of these agents so that the labelled complex appeared to interact with the aldehyde group of the collagen molecule while the phosphate moiety without the ^{99m}Tc-Sn moiety appeared to bind to bone mineral.

Unusual rates of osteoblastic activity have been implicated in influencing the uptake rates of radiolabelled bone-seeking agent (We69, Bl71). Observed increases in pyrophosphate uptake in patients presenting with osteomalacia has been explained by the observation that pyrophosphate is found close to immature collagen in the bone (Ka75, Ro76). Cox (Co74) indicated that the role of the complexing agents is that of a chelating agent to prevent colloid formation of the technetium-99m in its (IV) valence state and to allow direct incorporation of the element in this valence state into the bone.

Handmaker and Leonards (Ha76) report the clinical observation in which the ^{99m}Tc phosphate or phosphonate scintiscan produced early in the disease state manifests a "cold" lesion which later becomes "hot". Hoffer (Ho80) observed this early phenomenon seen with radiolabelled PO_4^- ion as the result of a tamponade of the blood vessels within the bone due to increased blood pressure inside the marrow cavity so that no overall increase in bone blood flow occurs. He further states that "the bone scan although very useful is neither as sensitive nor as specific as originally believed (Ho80). Since biodistribution of Ga-67 is not as dependent on blood flow as the Tc-99m phosphate complexes, Hoffer recommends a ^{67}Ga-citrate scintiscan procedure if the clinician suspects bone infection but no abnormal scintiscan is produced with a ^{99m}Tc-phosphate or phosphonate agent.

No differences in detection rate of bone lesions between the various phosphate and phosphonate complexes has yet been demonstrated (Du73).

No evidence can be found that phosphatase enzyme systems play a significant role in the localization of bone-seeking ^{99m}Tc phosphates or phosphonates and Rohlin et al. (Ro78) showed that tissues with high pyrophosphatase activity (intestinal mucosa, stratum intermedium, and subodontoblastic layers) did not show localization of ^{99m}Tc-pyrophosphate.

Subramanian et al. (Su75) reviewed blood and urinary clearance rates of technetium-99m phosphorous complexes in man. Methylene diphosphonate exhibited the fastest blood clearance rate which was very similar to that of ^{18}F. At six hours after administration EHDP blood clearance was less than that of MDP but more than that of MDP at 24

hours. Pyrophosphate showed slower blood clearance than either MDP or EHDP and polyphosphate demonstrated the slowest clearance rate of these four phosphorous agents. Fluorine-18 showed lower urinary clearance than all four phosphorous radiopharmaceuticals. MDP and EHDP exhibited similar clearance at 24 hours but MDP showed a higher clearance rate at 2 hours after intravenous administration. Polyphosphate and pyrophosphate demonstrated similar clearance rates within the 24 hour interval but less than that of MDP and EHDP. Subramanian et al. (Su75) presented the radiation dose estimates listed in Table 2.

The radiation absorbed dose estimates for EHDP and MDP were similar as were those for pyrophosphate and polyphosphate. For the listed organs, except bladder wall, the diphosphonates presented a lower radiation dose than the phosphates primarily because of slower renal extraction rates of the phosphates.

Because of the superior physical characteristics of Tc-99m (6 h T1/2, 140 Kev γ, and absence of particulate radiation, up to 14 mCi may be administered to an adult to produce a large photon flux which results in a high information density, minimizing statistical errors, and providing greater sensitivity than that realized with ^{85}Sr, ^{87m}Sr, and ^{47}Ca.

G. STUDIES RELATING RADIOGRAPHS AND BONE SCINTISCANS FOR DETECTION OF OSTEOMYELITIS

Weber et al. (We69) reported that the technique of radionuclide scintiscanning "is a sensitive diagnostic technique which can frequently indicate the presence and extent of lesions before they are visible on

Table 2

Radiation Absorbed Dose Estimates in Humans
(Rads/mCi)

(Subramanian, G, McAfee, JG, Blair, RJ, Kallfelz, FA, and Thomas, F.D: Technetium-99m-methylene diphosphonate - a superior agent for skeletal imaging: Comparison with other technetium complexes. J. Nucl. Med. 16: 744-755, 1975)

Organ	^{99m}Tc-EHDP or ^{99m}Tc-MDP	^{99m}Tc-pyrophosphate or ^{99m}Tc-polyphosphate
Skeleton	0.038	0.054
Red Marrow	0.025	0.038
"Average soft tissue"	0.009	0.013
Total Body (conventional)	0.007	0.010
Kidneys	0.031	0.047
Bladder wall	0.440	0.320
Liver	0.008	0.014
Ovaries	0.017	0.020
Testes	0.012	0.014

routine or special radiographs or tomograms". Handmaker and Leonards (Ha76) stated that scintigraphic techniques can produce positive results 10 to 14 days before such changes can be detected using radiographic techniques. Blair and McAfee (Bl76) stated that possibly one third of all patients with skeletal metastases had positive scintiscans and normal radiographs and less than one tenth had positive roentgenographs and normal scintiscans. Russin and Staab (Ru76) reported positive scintiscan results in a patient presenting with osteomyelitis several days before positive radiographic findings. Treves et al. (Tr76) presented data on 7 children presenting with osteomyelitis who all underwent scinitigraphic examination and demonstrated positive results. None originally demonstrated any radiographic abnormalities and only 3 eventually did so. Hamilton and Hurley (Ha79), however, reported a diagnostic accuracy of 56% for scintiscanning on a group of fourteen children presenting with osteomyelitis. Berkowitz and Wenzel (Be81) reported that in 7 children who presented with clinical signs and symptoms of osteomyelitis, radiographs and scintiscans with ^{99m}Tc methylene diphosphonate performed within 48 hours of admission were all reported as normal. Repeat scintigraphs 8-16 days after onset of symptoms showed confirmed signs of the disease process in four patients, while abnormal ^{67}Ga scintiscans were seen in two other patients, and a positive bacterial culture confirmed the seventh patient to have osteomyelitis. Gilday (Gi80) reported cases of osteomyelitis where delayed ^{99m}Tc bone-seeking radiopharmaceutical studies were diagnosed as normal but the blood pool image was not. Ash and Gilday (As80) reported poor results in diagnosing osteomyelitis in neonates using scintigraphic

techniques. Balsam (Ba80) presented a case report of a false positive scintigraphic study on a case of neonatal osteomyelitis. Handmaker (Ha80) indicated that there are problems associated with scintigraphic techniques when attempting to diagnose hematogenous osteomyelitis which will be reviewed in the discusssion portion of this thesis.

H. DYNAMIC UPTAKE IN BONE

Clinically used bone-seeking radiopharmaceuticals are administered intravenously whereupon the material rapidly distributes to various body compartments, mainly bone, while the nonbound component is excreted principally via the urine. Work has been done that suggests that short term uptake of commonly used bone-seeking radiotracers is closely correlated with blood flow to the bone and is relatively independent of osteogenesis (Ge74a). Other workers have produced results suggesting that while increased blood flow to a lesion produces more uptake, other factors have been alluded to which are thought to influence fixation at that site (Le76).

Another study (Si76) also indicates that regional blood flow primarily influences ^{99m}Tc-EHDP deposition in bone and also that altered regional radiotracer extraction efficiencies also play a role: these include blood flow, osteogenesis, metabolic activity, capillary permeability, volume of interstitial fluid, and bone surface area. Further work (Ga75) suggests that lesion-to-tissue ratio is influenced by changes in capillary permeability in the vicinity of the lesion.

^{99m}Tc-bone seeking radiopharmaceuticals studied clinically include polyphosphates, monofluorophosphate, diphosphonates, and pyrophosphate (Su76). Patients injected with ^{99m}Tc methylene diphosphonate are normally imaged with a gamma camera two hours after injection of the radiopharmaceutical because images obtained after this time interval are equivalent to a 3-4 hour scintiscan with ^{99m}TC pyrophosphate or EHDP or a 4-5 hour scintiscan with ^{99m}Tc-polyphosphate (Su76).

I. ^{67}GA CITRATE AND INFLAMMATORY LESIONS

^{67}Ga citrate is a bone-seeking radiopharmaceutical which concentrates in normal bone and marrow and is used diagnostically for tumor imaging and detection of inflammatory lesions (Ha78, Ro79). Its use in tumor imaging is outside the scope of this thesis so discussion will be confined to detection of inflammatory lesions.

The mechanisms of uptake of ^{67}Ga by inflammatory lesions are not fully understood but Hoffer has recently published two papers on this subject (Ho80, Ho80a) in which he associated uptake of ^{67}Ga with (1) *in vivo* leukocyte radiolabelling, (2) lactoferrin binding at the site of infection, (3) direct bacterial uptake, and (4) siderophore-^{67}Ga complex formation at the inflammatory site which is then transported into the bacteria. Menon *et al.* (Me78) and Shysh *et al.* (Sh80) also reported direct uptake of radiogallium by microorganisms. Shysh *et al.* (Sh81) reported that the macrophages within a liver granuloma of a mouse treated with BCG are associated with the bulk of the ^{67}Ga found in the lesion. Tzen *et al.* (Tz80) reported that either increased capillary permeability or iron-binding proteins may produce regional

accumulation of radiogallium and presence of either or both of these factors at sites of inflammation may be involved in uptake of the radiotracer in inflammatory foci. An exhaustive review of gallium localization as pertaining to nuclear medicine procedures has been published recently (Fr78).

Handmaker and Leonards first proposed the use of ^{67}Ga to accompany the bone scintiscan in diagnosing joint infection and osteomyelitis (Ha76, Ha76a). Hoffer (Ho80) has reported that a problem inherent with the ^{99m}Tc phosphate scintiscan is that an early inflammatory lesion in bone may tamponade the blood vessels with the bone and so prevent increased blood flow within the bone and that ^{67}Ga is more effective as a diagnostic agent because it is less affected by blood flow. Hoffer further states that "when infection is suspected and the Tc-99m phosphate bone scan is negative, a Ga-67 scan is often indicated" (p. 486). Rosenthall et al. (Ro79) (p.718) state "^{67}Ga concentration in bone per se may reflect not inflammation but increased bone metabolism in response to trauma, and thus it is necessary to supplement the ^{67}Ga examination with a ^{99m}Tc-PP study to assess the relative distribution patterns. If they are incongruent, osteomyelitis is likely, but if they are congruent infection is in doubt". Incongruence is due to the fact that radiogallium is a bone-seeking radiotracer which produces a scintiimage of the bone in the same manner as other bone-seeking radiopharmaceuticals but in addition if an inflammatory lesion is present, the ^{67}Ga-citrate scintiscan will show the image of the bone as well as uptake by soft-tissue involvement, direct bacterial uptake, and the other factors discussed earlier in this section. Furthermore, the authors

cautioned that interpretation of ^{67}Ga scintiscans must be done bearing in mind the clinical vageries associated with radiogallium.

J. ^{18}F-FLUORIDE UPTAKE BY BONE

Wootton (Wo75, Wo74) reported that the single passage extraction of ^{18}F-fluoride in rabbit bone is approximately 100% and postulated that increased bone uptake of this radiotracer simply reflects increased bone blood flow. King et al. (Ki76, Ki77) stated that blood flow produced greater effect on deposition of ^{18}F-fluoride on bone than variations of exchangeable bone pool. Costeas et al. (Co71) produced data which indicated that uptake of ^{18}F-fluoride by bone occurred via exchange of ^{18}F-fluoride with stable fluoride on the surface of the bone crystal and not with hydroxyl ions in hydroxyapatite as was generally accepted to that time.

Ackerhalt et al. (Ac74) compared ^{99m}Tc-Sn-polyphosphate, Sn-1-hydroxyethane-1-diphosphonate (EHDP), and ^{18}F-fluoride and concluded that the faster blood clearance rate of ^{18}F and more rapid uptake by the skeleton make it a superior agent when compared to the ^{99m}Tc-phosphorous compounds.

Charkes et al. (Ch75) developed a four compartmental model to fit human kinetic data and later described a five compartment model for ^{18}F-fluoride uptake in humans (Ch78) which behaves in a nonlinear manner in that a five fold simulated increase in skeletal or systemic blood flow produced no appreciable bone uptake of fluoride but a simulated increased rate of bone extraction produced a notable change in uptake.

Charkes et al. (Ch79) using this five-compartment model to study fluoride kinetics in rats found good agreement between their experimental estimates of fluoride partition between bone ECF and bone substance for 0.5-2 minutes and 1 hour after injection. These workers also reported migration of the radiotracer within the bone tissue after the animals' deaths which they suggested might be due to fluoride movement between "bone substance" and bone extracellular fluid (Ch79).

Creutzig (Cr75) reported a series of 75 patients with total hip replacement comparing ^{99m}Tc-EHDP and ^{18}F and found similar uptake ratios between infected and normal contralateral femur for both radioisotopes. Evaluation of the ^{99m}Tc-EHDP scintiscans produced 4 false positive results while the same 4 patients all produced normal ^{18}F scintiscans. No false negative scintiscans were seen. In 18 patients both series of scintiphotos were negative. Riggins et al. (Ri74) reported use of ^{18}F in dogs to study uptake in the femoral head and concluded that localization of the radiotracer was directly correlated with blood flow in the bone. D'Ambrosia et al. (Da75) reviewed 75 patients with avascular bone disorders who underwent ^{18}F scintigraphic procedures correlated with clinical findings, radiographs, and when possible ^{99m}Tc-tetracycline scintigraphy and histological examinations. The authors reported that uptake by the femur of radiofluoride accurately reflected the degree of vascularization of the bone in these patients and that in 25 of these 75 patients with femoral neck fractures, the ^{18}F distribution correlated with radiolabelled tetracycline uptake and verified that ^{18}F uptake accurately reflects blood flow to bone.

K. BONE MARROW SCINTISCANNING

Because of the close relationship between bone and bone marrow, an evaluation of the bone marrow can be employed in the study of diseased bone. Bone marrow has been classified as either red or yellow. Red marrow is hematologically active and is the site of erythropoiesis, granulopoiesis, thrombocytopoiesis and the reticuloendothelial system in the bone while yellow marrow is fat and has no such functions associated with it. However, in cases of bone marrow extension yellow marrow is converted to red marrow (Ga69).

McIntyre (Su76a) stated her belief that no one radiopharmaceutical is adequate by itself to clinically image the functioning bone marrow sites of haematopoiesis. Various radiocolloids have been used to delineate sites of marrow function but these agents, however, are also accumulated by the reticuloendothelial cells of the liver and spleen. Particle ingestion by the RES is a function of "fixed" macrophages which line the blood sinuses of the lung, spleen, liver and bone marrow (Su76a). Greenberg et al. (Gr66) reported that 96% of radiocolloid injected into the dog is distributed to the liver and spleen and 2.8% is localized within the bones, thus the marrow in the spine behind these organs cannot be adequately studied with this approach (Gr66, Zi52).

Various radiopharmaceuticals have been used in the study of marrow function including ^{198}Au colloid (Zi52), ^{52}Fe-ferrous citrate and ^{59}Fe-ferrous citrate (Va64). ^{99m}Tc sulphur colloid (Me75), ^{99m}Tc-phytate (Eg79, Su73), ^{99m}Tc-antimony sulphur colloid (Eg79, Ma80a), and ^{113}In colloids (Ta74). ^{99m}Tc colloids readily delineate the functioning reticuloendothelial portion of the bone marrow, are relatively

inexpensive, easily obtainable, present a relatively small radiation dose to the patient, and enable a full study to be executed in one session. Subramanian et al. (Su73) suggested that ^{99m}Tc stannous phytate had potential use as a reticuloendothelial system imaging agent but Hamilton et al. (Ha77) showed that compact bone rather than bone marrow was the site of accumulation of this radiotracer if in vivo incubation was employed.

Bone marrow imaging radiopharmaceuticals should possess the following characteristics: (1) diameter of the labelled colloid must be less than 50 mμ (Ma80a), (2) possess a high zeta potential to effect a more stable colloid which, in turn, results in the full potential to be distributed in the body (Su76), (3) an appropriate number of colloid particles so as not to overwhelm the phagocytic ability of the system and thus avoid the phenomenon in which particle clearance rate becomes less affected by rate of systemic blood flow (Su76b), (4) appropriate surface characteristics of the colloid particles, (Su76b), (5) opsonization or the coating of these particles by opsonin, a substance similar to an antibody so that phagocytosis of the particle-opsonin complex occurs (Su76b). Several techniques have been reported to determine particle size of ^{99m}Tc sulphur colloid (Wa77, Kr76, Bi79, Li79, Wa79) and all reports have stated that the diameter of most sulphur colloid particles is greater than 100 mμ and extends over a broad range. Martindale et al. (Ma80a) stated that ^{99m}Tc antimony colloid is a better bone marrow imaging agent in rabbits than ^{99m}Tc sulphur colloid but did not report which of the previously mentioned factors was responsible for greater uptake. Takahashi (Ta74) reported on ^{113m}In colloidal preparations incorporating chondroitin sulfate or

chondroitin polysulfate and reported superior marrow to liver ratios than those obtained with ^{198}Au colloid and ^{99m}Tc sulphur colloid

Feigin (Fe74) reported data from a rabbit model for osteomyelitis in which he studied bone marrow uptake of ^{99m}Tc sulphur colloid as a potential means of early diagnosis of osteomyelitis. Of 6 infected animals, all demonstrated less uptake in the affected limb as compared to the contralateral normal limb at least four days before radiographic differences were observed.

L. ^{99m}Tc-SULPHUR COLLOID LABELLED GRANULOCYTES

Granulocytes may be labelled in vitro by incubation with ^{99m}Tc sulphur colloid (Le76a, An75, En75). Following intravenous injection, these radiolabelled leukocytes localize at inflammatory lesions affording detection by a gamma-scintillation camera (Le76a, Uc73, Ba77). This approach to localization of inflammatory foci has been applied to lungs (An75), intestine (Ba77), and bone (Le76a).

III. MATERIALS AND METHODS

A. EXPERIMENTAL ANIMALS

A modification of the ostemyelitis animal model developed by Norden (No70) was used in this project. Male New Zealand white rabbits weighing 2-3 kg were anesthetized with sodium pentobarbital, 2.5mg/kg i.p. and both legs were clipped of hair, shaved, and cleansed with a solution of 70% ethyl alcohol. Under ether anesthesia a 20 gauge 1 inch disposable aluminum needle was introduced into the medullary cavity of the tibia by passing it percutaneously through the lateral aspect of the metaphysis. Into the medullary cavity of the right tibia was injected 0.1 ml of 5% Sodium Morrhuate Injection USP (Eli Lilly Co.), then 0.1 ml of bacterial suspension, followed by 0.1 ml of sterile normal saline to flush all the sclerosing agent and bacterial suspension into the bone. The needle was then removed and the skin again disinfected with the alcoholic solution. In a similar manner the left (control) leg was injected with 0.1 ml of the sodium morrhuate solution followed by 0.2 ml of sterile saline. During the experiment the animals were housed separately in rabbit cages and supplied with water and rabbit food ad libitum. The temperature in the animal room was kept constant at 22°C with alternating 12 hour periods of light and darkness.

B. MICROORGANISMS

The bacteria used in all experiments were the standard laboratory strain of Staphylcoccus aureus phage type 47 obtained from the laboratories of Dr. F. Jackson, Department of Medical Bacteriology, Faculty of Medicine, University of Alberta. The bacteria was supplied as a suspension in sterile normal saline and was assayed just prior to

injection and adjusted to concentrations varying from 2×10^9 to 10×10^9 bacteria per ml.

C. RADIOPHARMACEUTICALS AND REAGENTS

1. ^{99m}Tc Pyrophosphate

The ^{99m}Tc labelled pyrophosphate used in the initial portion of this work was supplied by the Department of Nuclear Medicine, Cross Cancer Institute, Edmonton, Alberta and was composed of tetrasodium pyrophosphate, stannous chloride, hydrochloric acid, sodium hydroxide, and sterile water for injection USP. The radiochemical purity of all the ^{99m}Tc pyrophosphate supplied was greater than 95% as assayed by thin layer chromatography (Gelmand ITLC® S.G.) with butanol as a solvent for determination of unbound pertechnetate and 0.9% sodium chloride as another solvent system for determination of insoluble radiocolloid.

2. ^{99m}Tc Methylene Diphosphonate

All ^{99m}Tc methylene disphosphonate used in this investigation was prepared in kit form according to the following protocol using chemicals and reagents of A.C.S. or analytical grade quality: To make 100 kits:

CHEMICAL	AMOUNT
Methylene Diphosonic Acid (Sigma® Chemical Company)	1.0 g
Ascorbic Acid Injection (Winthrop)	100 mg
Stannous Chloride Dihydrate (Mallinckrodt Chemical Works)	100 mg
1N HCl (Anachemia Chemicals Ltd.)	4 ml
1N NaOH (Anachemia Chemicals Ltd.)	as required
Sterile Water for Injection USP (Baxter Laboratories of Canada Ltd.)	Q.S.

The methylene diphosphonic acid and ascorbic acid injection USP were dissolved in 50 ml sterile water for injection USP. The stannous chloride dihydrate was dissolved in 4 ml of 1N HCl and was added dropwise with stirring through a 0.22 μm Millipore® filter to the methylene disphosphonic acid solution. This solution was then stirred for another five minutes. The pH was adjusted to 6.2 with 1N NaOH. A sufficient volume of sterile water for injection was added to make a final volume of 100 ml. One ml portions were then dispensed through a sterile 0.22 μm Millipore® filter into sterile, sealed vials. The kits were then immediately frozen and stored at -4°C. When required, the kits were reconstituted with approximately 6.0 ml of ^{99m}Tc-sodium pertechnetate. Sterility tests were conducted on these kits by the Department of Bacteriology, University of Alberta Hospital, Edmonton, Alberta.

The technetium-99m used to label these kits was obtained from ^{99}Mo-^{99m}Tc radionuclide generators (New England Nuclear, Boston, Mass., U.S.A.) supplied to the Edmonton Radiopharmaceutical Centre. Radiochemical purity assay of the final radiopharmaceutical consisted of chromatography on Gelman® ITLC S.G. with n-butanol for determination of unbound pertechnetate and with normal saline for determination of insoluble radiocolloid. The chromatograms were developed for 10 cm and then analyzed on a chromatogram strip scanner. The radiochemical purity was routinely greater than 95% and the radiopharmaceutical was prepared just prior to injection.

3. Macroaggregated Human Serum Albumin

Macroaggregated human serum albumin was made according to the following formulation:

CHEMICAL	AMOUNT
Human Serum Albumin (25% w/v) (Connaught Medical Research Laboratories)	0.8 ml
Sodium Acetate (Fisher Scientific Company)	2.0 g
Sterile Water For Injection USP (Baxter Laboratories of Canada Ltd.)	100 ml

The sodium acetate was dissolved in sterile water for injection (10 ml) and to this was added 0.8 ml of human serum albumin. This solution was then passed through a 0.22 µm Millipore® filter into a sterile 125 ml vial containing a magnetic stirring bar. Sterile water for injection (19 ml) was also added into the vial which was then placed into a hot water bath at 77°C on a combination hot plate-magnetic stirrer (Cole-Parmer Model No. 4817) equipped with an external temperature probe. The temperature was maintained after it dropped to 72°C. The contents of the vial were continously stirred until the liquid turned milky in appearance indicating the formation of macroaggregates (approximately 90 minutes). The vial was allowed to cool to room temperature and then centrifuged at 2400 rpm for 10 minutes on a Damon/IEC Division model CU-5000 centrifuge after which the supernatant was carefully withdrawn through a 4 inch long spinal needle into a 5 ml syringe. Particle size was assayed microscopically on a hemocytometer grid and found to be as follows: over 90% were in the range of 10-50 microns and no particles were over 100 microns. This preparation was carried out under aseptic conditions and the final suspension of albumin macroaggregate adjusted to contain about 1×10^7 particles per ml was supplied to the medical bacteriology laboratory to act as a medium for the inoculating bacteria.

4. ^{99m}Tc-Labeled White Blood Cells

The following procedure was used for labelling rabbit white blood cells with ^{99m}Tc: A 10 ml sample of blood was collected from a rabbit into a heparinized sterile syringe by cardiac puncture and transferred to a sterile siliconized vacutainer containing 500 units of sodium heparin. One-half ml (20 mCi/ml) of technetium-99m sulphur colloid, supplied by the Department of Nuclear Medicine, Cross Cancer Institute, Edmonton, Alberta, was added to the tube with mixing followed by incubation for 30 minutes at 25°C on a rotator. The tube was then centrifuged at 1400 rpm for 10 minutes and the plasma was removed using an 18 G, 3 1/2 inch sterile spinal needle and a 20 ml sterile syringe. The cells were then resuspended in a 1:1 mixture of sterile saline for injection: ACD solution and then centrifuged at 1400 rpm for 20 minutes. The supernatant was withdrawn using a spinal needle and the cells were resuspended in 3 ml saline for injection. The labelled blood cells were transferred to another sterile vacutainer through a 100 μm sterile filter to remove any clotted particles. The final suspension of blood was assayed in an isotope dose calibrator and 3.0 ml containing 500 μCi was reinjected into the animal via an ear vein. The rabbit was then imaged three hours post-injection on the Nuclear Chicago Pho/Gamma III gamma camera.

5. Gallium-67 Citrate Distribution Study

The Department of Nuclear Medicine, Cross Cancer Institute supplied 1.0 mCi of gallium-67 citrate for a tissue distribution study on an osteomyelitis-positive rabbit. The gallium citrate was injected in a volume of 0.3 ml via a marginal ear vein. Forty-eight hours post-injection the animal was sacrificed and a series of tissue samples

including: whole blood, plasma, lymph, spleen, kidney, adrenal, normal thigh tissue, muscle peripheral to diseased bone, contents of control tibia, diseased bone marrow (no pus), diseased bone pus, bone mineral from control leg, bone joint of control leg, bone mineral from diseased leg, small intestine, liver, total monocyte sample from whole blood, and red and white blood cells from whole blood samples were collected and assayed for radioactivity on a Searle model 1195 gamma spectrometer.

6. ^{18}Fluorine

^{18}Fluorine as Na^{18}F was provided for this experiment by Dr. L.I. Wiebe of the Division of Bionucleonics and Radiopharmacy, Faculty of Pharmacy and Pharmaceutical Sciences, University of Alberta. The ^{18}F was produced in the Slowpoke nuclear reactor by irradiating 20 mg of ^{6}Li ($LiNO_3$) in solution for 2 hours in the neutron flux to form the following reaction:

$$^{6}Li\ (n, \alpha)\ ^{3}H.$$

The ^{3}H produced by the above nuclear reaction then underwent a recoil reaction (2.7 MeV) in the following manner:

$$^{16}O\ (^{3}H, n)\ ^{18}F.$$

The solution was boiled to dryness, then redissolved in water, and this procedure repeated twice again to remove any ^{3}H contamination.

An osteomyelitis-positive rabbit was anesthetized with sodium pentobarbital (2.5 mg/kg) i.p. and Innovar® Vet (0.1 ml/kg) i.m. The anesthetized animal was then injected with 53 μ Ci of ^{18}F in a volume of 4.7 ml via a marginal ear vein, positioned under the Nuclear Chicago Pho/Gamma III gamma camera and Positron III head for a series of bone scans at various time intervals.

D. RADIOLOGY

The radiograms were made using a Faxitron® 804 X-ray unit, Picker X-ray cassettes, and Cronex® and Cronex® 2 DC Medical X-Ray Film (10 x 12 inches). A special rabbit holding-board was constructed of pegboard, wooden pegs, elastic bands, Velcro® strips, and Plexiglass® in order to hold the rabbits motionless under the X-ray tube in the proper position so that the tibiofibula complex was fully visible in the roentgenograms. With this arrangement it was possible to duplicate the positioning of each animal. The X-ray unit was modified so that the X-ray tube could be energized by remote control with the door in the open position thus allowing the rabbits' hind legs and X-ray cassette to be placed directly under the X-ray tube. The loaded cassette was placed on the holding-board and then the rabbit was anesthetized with Nembutal Sodium (2.5 mg/kg) i.p. and Innovar® Vet (0.08 mg/kg) and placed on the cassette with its hind legs properly positioned. Because the cassette was directly below the animal, no shadows from the holding-board appeared on the radiogram. A one-second exposure was made at 46 kVp. This was the shortest exposure time possible on this equipment. No filters were required between the X-ray tube and the animals. Roentgenograms of the rabbits were made prior to inoculation with the bacteria (to serve as a control), immediately following the inoculation procedure (to check for bone trauma), and on a regular basis thereafter (to follow the progression of the disease state). At the end of an experiment, these radiograms were independently evaluated by practising radiologists at the Department of Nuclear Medicine, at the Cross Cancer Institute, Edmonton, Alberta. The rabbit identification number and date on each film was identified only by a random code number. Each leg on

the radiogram was evaluated according to the following criteria: (1) normal or abnormal and (2) if abnormal, was the difference a result of (a) trauma or (b) ostemyelitis? The completed evaluation forms were decoded and the raw data was charted on a time scale to indicate the time of onset of observed bone changes.

E. BONE SCANS

Immediately following X-ray, each rabbit was injected intravenously with 700 μCi of bone scanning agent (either pyrophosphate or methylene diphosphonate) labelled with technetium-99m in a total volume of 0.1 to 0.2 ml. After an appropriate waiting period (three hours for pyrophosphate and two hours for methylene diphosphonate), the rabbits were anesthetized and placed in the same position as used for X-ray on the animal holding board. A Nuclear Chicago Pho/Gamma III gamma camera and Polaroid film Type 667 were used to record all bone scans of the rabbits' hind limbs. Routinely 300,000 counts were accumulated for each view. Each bone scan was coded in exactly the same manner as the radiographs and was independently evaluated as normal or abnormal by the same group of radiologists.

F. INVESTIGATIONAL PROCEDURES

1. Dynamic Uptake Studies

In this experiment the levels of radioactivity in the blood, infected leg, and control leg of each animal were monitored by a multiprobe system coupled to a multichannel analyzer immediately following the intravenous injection of ^{99m}Tc-methylene diphosphonate. Matched NaI (Tl) gamma scintillation detectors (19 mm diameter) were

placed in 9 mm thick cylindrical lead collimators with the detector face withdrawn 25 mm into the lead collimator to limit the field of view of each detector. Each detector was connected to an Ortec® model 486 (Ortec Incorporated, Oak Ridge, Tennessee, U.S.A.) pulse height analyzer and the inputs fed into a Nuclear Chicago model 25601 (G.D. Searle, Des Plaines, Illinois, U.S.A.) multichannel analyzer. Three such probes were carefully matched and calibrated to record the 140 Kev emissions from Tc-99m.

Each rabbit was anesthetized with Nembutal® and placed on a specially constructed platform with one probe placed under the proximal end of the tibia of the right leg (infected leg), another probe under the same area of the left leg (control leg), and another probe over the right ear to measure blood levels of radioactivity. With the animal in position, the background levels of radioactivity were recorded for about 30 seconds, the 0.1 ml of Tc-99m methylene diphosphonate (specific activity 1.0 mCi/ml was injected via an ear vein (left ear) and the levels of radioactivity under each detector were monitored continually up to two hours post-injection. The output from each detector was presented on a Franklin printer (Franklin Electronics, Bridgeport, Penn., U.S.A.) series Franklin Electronics Series 1200 Hi-Speed Parallel Printer, model 4428(60 seconds per channel), on an X-Y plot recorder, and on punched tape for further analysis.

2. Radio-activity Uptake Studies

In an attempt to quantitatively assess the uptake of Tc-99m - methylene diphosphonate in the infected and control leg, a series of experiments was undertaken using a specially constructed single probe counting apparatus.

In this study, one 50 mm diameter NaI (Tl) scintillation crystal was placed within a 10 mm thick cylindrical lead collimator with its detector face withdrawn a distance of 25 mm from the open end of the collimator. This assembly was then placed under a specially constructed small table provided with an overlying 2 mm lead shield with the crystal surface facing upward through a hole drilled through the table top and shield. The output from the crystal and preamplifier was fed to a BNC Portanim® model AP-2 bin, an Canberra® high voltage power supply model 3002, an Ortec® model 486 pulse height analyzer.

The rabbits were injected intravenously with 0.1 ml of Tc-99m MDP (specific activity 800 μCi / ml) and under sodium pentobarbital anesthesia, the rabbit was carefully placed on the shielded table top so that the proximal end of the tibia was across the face of the collimated detector. Triplicate one-minute counts at 30 and 60 minutes following Tc-99m MDP injection were made of the control and infected legs.

IV. RESULTS AND DISCUSSION

During the course of this investigation it became evident that a realistic animal model was necessary to evaluate the efficacy of bone scintigraphy versus roentgenology for early detection of osteomyelitis. Excessive bone trauma during injection would either be visible on X-ray or show as a positive bone scintiscan. A large amount of sclerosing agent would change interior bone architecture and complicate the interpretation of radiograms. Induction of a localized bone infection required a virulent bacterial strain in that species and only sufficient numbers of bacteria to cause infection without producing general sepsis. The following sections indicate the experiments that were done to evaluate various methods of inducing osteomyelitis in animals.

A. DEVELOPMENT OF AN ANIMAL OSTEMYELITIS MODEL

1. Rabbit Model for Osteomyelitis

Preliminary investigation using procedures as outlined by Norden (No70) indicated that induction of osteomyelitis in rabbits could not be readily duplicated in this laboratory without some modification. By varying both the number of bacteria, and volume of sclerosing agent injected, it became apparent that three factors were of major importance in producing osteomyelitis in the rabbit: (1) use of a particular strain of Staphylococcus aureus that was virulent in the species, (2) use of a sclerosing agent, and (3) utilization of young rabbits whose bone is sufficiently soft to allow penetration of a hypodermic needle into the medullary cavity of the tibia without causing excessive trauma. After several unsuccessful attempts using different strains of Staphylococcus including that cultured from a case of human osteomyelitis, it was finally found that the laboratory strain phage

type 47 obtained from the Department of Medical Bacteriology, Faculty of Medicine, University of Alberta, Edmonton, Alberta could produce the desired disease process. Further experiments showed that 0.1 ml of bacterial suspension could be used optimally if the assay of colony-forming units ranged between 2×10^9 to 9×10^{10} per ml.

The total injection volume was restricted in the small rabbit because volumes larger than 0.3 ml introduced into the medullary cavity of the tibia were found to produce an infection in the entire cavity rather than being localized at the injection site. It was also determined that the bacteria must be injected directly into the medullary cavity of the bone and also that sodium morrhuate must be injected into the cavity at the time of innoculation for the infection to occur. While the injection of bacteria in the range of about 7×10^9 colony-forming units was adequate to induce the infection, if the inoculating suspension was of a higher assayed concentration, bacteria would be found upon post-mortem examination not only in the bones but also in the liver, gall bladder, and bloodstream as well. The difficult problem of selecting a strain of bacteria which is virulent in the rabbit and would produce osteomyelitis without sepsis was also noted by other investigators (Fe77). In the young rabbit, a 20 gauge needle can readily be inserted through the tibia into the medullary canal. Heavier, 16 gauge needles were tried but these left puncture holes which could be visible on radiographs and occasionally produced positive bone scintiscans.

It was found through trial and error that a suspension of Staphylococcus aureus, by itself, flushed into the medullary cavity did not produce a bone infection. Osteomyelitis occurred only if sodium

morrhuate was also introduced along with the bacteria. The sodium morrhuate in the medullary cavity effectively occluded the blood vessels entering and leaving the medullary space and so produced a closed environment which presented the bacteria with the necessary requirements to establish itself. Furthermore, restriction of the blood circulation in the region of the sodium morrhuate injection site could prevent leukocyte migration to the site of infection.

2. Controls

Interpretation of the radiographs was complicated by the uncertain effects which were produced by the sclerosing agent and even by the trauma of injection on the appearance of the radiographs. To facilitate evaluation of the radiographs, a series of controls were prepared in the following manner: in three rabbits, only the right tibia was injected with 0.1 ml of sodium morrhuate and 0.05 ml saline while leaving the left leg intact for comparison. Radiographs and bone scans were then performed daily for two weeks. These served as controls for the effects of sclerosing agent only. In another three rabbits, the right tibia was injected with 0.1 ml of sodium morrhuate and 0.05 ml saline and the left injected with 0.15 ml of saline only. Daily roentgenographs and bone scans were performed to monitor the effects of sclerosing agent, saline, and the trauma of the inoculating procedures. This series of radiograms and scans were made available to the radiologists as references for evaluating the experimental radiographs and bone scintiscans.

During the course of the experiments, the control leg was routinely injected in the identical manner with the omission of the bacteria.

Therefore, both limbs were exposed to the same injection trauma, sclerosing agent, and saline.

3. Osteomyelitis Model Using Bacterially Impregnated Macroaggregated Human Serum Albumin

In an effort to reduce the artefacts on the roentgenographs due to the sclerosing agent, an attempt was made to modify the induction process of osteomyelitis by using macroaggregated human serum albumin as a medium for bacterial growth and injecting bacteria as a suspension within the macroaggregate along with reduced quantities of sodium morrhuate. The prepared albumin macroaggregates were supplied to the Department of Medical Bacteriology, Faculty of Medicine, University of Alberta, Edmonton according to the formulation and volume previously described. Normally, as an integral part of the formulation stannous chloride is included to act as a reducing agent to enable the macroaggregated albumin to be labelled with technetium-99m. However, the tin was excluded from this preparation to avoid any potential influence on the growth of bacteria in this medium.

The inoculating bacteria were grown in a medium consisting of 2.0 ml of the suspension of the macroaggregate (1×10^7 particles / ml) and 2.0 ml of nutrient broth. The Staphylococcus aureus grew successfully in this medium but did not reproduce sufficiently to reach as high a final assay concentration as did the same inoculating volume in neat nutrient broth (8.5×10^8 vs 2×10^9 colony forming units/ml). The suspension containing the macroaggregates and nutrient broth was then injected into the right tibia of the animals along with varying volumes (ranging from none to 0.1 ml) of sodium morrhuate.

For comparison of this bacterial media a second inoculating suspension of bacteria was prepared in the usual way, i.e.: grown in nutrient broth, washed, resuspended in normal saline, assayed. and adjusted to bacterial number.

Table 3 indicates the production of ostemyelitis by these two procedures.

The four rabbits which were inocculated with the customary bacterial suspension all developed osteomyelitis as evidenced by radiography and gamma scintigraphy. However, the four rabbits inoculated with the bacterial suspension containing the macroaggregates demonstrated that the disease state could be induced using lesser amounts of sclerosing agent, but that injection of the bacterial impregnated macroaggregates alone would not cause an infection. Preliminary work on this project indicated that a sclerosing agent was necessary to induce osteomyelitis. This protocol showed that lower volumes of sodium morrhuate were sufficient to produce the model but that some sclerosing agent was necessary. This experiment suggested that the vascular network of the tibia in an impaired state is less capable of resisting infection than in its normal state. The deposition of as small a volume as 0.03 ml of sodium morrhuate within the medullary cavity was sufficient to alter the vascular network of the bone, enabling the bacteria to successfully invade the bone.

This phenomenon can be explained if consideration is given to the anatomical structure of the rabbit tibia. It has been shown that the afferent nutrient capillaries of the epiphyseal growth plate change direction abruptly and enter the venous network of the medullary cavity via a complex of large sinusoidal veins characterized by sluggish blood

TABLE 3

OSTEOMYELITIS POSITIVE RABBITS

RABBIT NO.	RT. LEG		EXPERIMENTAL LEG EVALUATED POSITIVE EITHER BY SCAN OR RADIOGRAPHY AND DAY EVALUATED AS POSITIVE	
			DAY AFTER INOCULATION*	
			SCAN	X-RAY
3	0.10 ml NaMorr 0.10 ml ISA 0.05 ml SNS	+	RT - Never LT - Never	RT - Day 6 LT - Never
4	0.10 ml NaMorr 0.10 ml ISA 0.05 ml SNS	+	RT - Day 3 LT - Never	RT - Day 0 LT - Day 2
5	0.10 ml NaMorr 0.10 ml ISA 0.05 ml SNS	+	RT - Day 4 LT - Day 9 only	RT - Day 3 LT - Day 3
6	0.10 ml NaMorr 0.10 ml ISA 0.05 ml SNS	+	RT - Never LT - Never	RT - Day 3 LT - Day 3
7	0.10 ml NaMorr 0.10 ml ISB 0.05 ml SNS	+	RT - Day 9 LT - Never	RT - Day 6 LT - Day 7
8	0.05 ml NaMorr 0.10 ml ISB 0.10 ml SNS	+	RT - Never LT - Never	RT - Day 3 LT - Never
9	0.03 ml NaMorr 0.10 ml ISM 0.12 ml SNS	+	RT - Never LT - Never	RT - Day 3 LT - Day 9
10	No NaMorr 0.10 ml ISB 0.15 ml SNS	-	RT - Day 4 only LT - Never	RT - Never LT - Never

NaMorr = sodium morrhuate
ISA = Inoculating Suspension of Bacteria only (2×10^9 colony-forming unit/ml)
ISB = Inoculating Suspension of MAA and Bacteria (8.5×10^8 colony-forming unit/ml)
SNS = sterile normal saline

* - animals observed by scintigraphy and radiography up to 14 days after inoculation

flow (Wa70). Hematogenous infection of this aspect of the bone has been shown to occur easily in young rabbits (Wo70). The metaphysis does not seem to have the ability to defend itself against infection. This can be explained by several factors. The cells lining the capillary to the metaphysis lack phagocytic ability and while the efferent loop possesses such cells, they are inactive (Wo70). Furthermore, because the ascending loop of the capillary is of a single structure and possesses a diameter of approximately eight microns and the descending portions are often multiple and usually possess diameters of fifteen to sixty microns, the descending loop blood flow is characteristically torpid (Br59). Moreover, in the region of the epiphyseal growth plate, the capillary loops are nonanastomosing and so any occulsion caused by such objects as bacteria or macroaggregates would produce a locus of avascular necrosis (Mo59). The predisposing situation presented by these factors for the disease process is enhanced further if the milieu is modified by the deposition of sclerosing agent within the medullary cavity. At least part of the vascular network servicing the bone would be occluded, thereby decreasing the normal defence mechanism of mobilizing leukocytes at the site of infection and so favoring the virulent bacteria inside the bone with an environment more suitable for reproduction. This occlusion would produce a decreased rate of blood flow through the bone enabling the fixation of bacteria to the walls of the medullary cavity or vascular system of the bone.

Bacteria present in a vascular bundle within the bone characterized by a restricted flow rate could more readily lodge in situations where capillaries change directions or in nonanastomosing

single structure capillaries. If so lodged, even a single bacterium could potentially replicate and produce a focus of infection.

4. Cat Model for Osteomyelitis

Post mortem examination of the osteomyelitis-positive rabbits revealed that the infected tibiae were filled with an almost solid, cheeselike pus. This condition contrasts with the human disease state in which the pus is less viscous. Consultation with the resident veterinarians of the Department of Histopathology, Veterinary Services Division, Alberta Agriculture, Edmonton led to the suggestion that cats should be tested as an alternate to the rabbit model because past clinical observations of bone pus in that species were of a lower viscosity. Two female cats of approximately five months of age were inoculated with bacteria and sclerosis agent in a manner identical to that used for rabbits. However, observations over three weeks by radiograph and bone scan failed to indicate any signs of osteomyelitis. It was concluded that this strain of Staphylococcus was not virulent in cats and no further attempt was made to pursue this model.

5. Alternate Rabbit Model for Ostemyelitis

In a series of preliminary experiments, an attempt was made to establish a rabbit osteomyelitis model which would avoid the trauma of bone puncture at the injection site. The hind limbs of three rabbits were surgically prepared and under pentobarbital (3 mg/kg i.p.) and ether anesthesia a straight incision about two inches long was made from the metaphysis along the diaphysis on the inner aspect of the tibia. Underlying fat and muscle were carefully separated and a hole was drilled midshaft using a hand drill and a sterile 1 mm diameter bit. A sterile cannula was inserted through the hole and the tip advanced into

the proximal metaphysis of the tibia and the other end left buried under the skin. The incision was closed with running 3-0 chromic catgut sutures. The rationale behind this approach was that following healing from this surgery, a bacterial suspension and sclerosing agent could be injected via the catheter into the metaphysis without the accompanying trauma of bone puncture. Unfortunately, the bone scintiscans showed that the area of the drilled hole at midshaft was consistently positive from the time of surgery until at least three months later. Since such a persistent "hot" spot on the bone scan could interfere with a positive osteomyelitis scan, this approach was abandoned.

B. HISTOPATHOLOGICAL EXAMINATIONS

Dr. R.J. Lewis, D.V.M., and Dr. G.R. Johnson, D.V.M., Head, Histopathology, Veterinary Services Division, Alberta Agriculture, O.S. Longman Building, Edmonton, Alberta kindly performed the histopathological examinations and reported on lesions found in the rabbits used in these experiments. The rabbits were delivered alive to the laboratory and were killed immediately prior to the post mortem examination. Both the left and right tibia were sectioned identically and the lesions which were found in each rabbit were reported. The lesions seen in the diseased tibiae of these rabbits were all similar. The changes seen were summarized as follows: The area beneath the epiphyseal plate had undergone a severe necrotizing reaction. The predominate change was lysis of bone. These areas of necrosis were surrounded by fibrous tissue proliferation. The periphery of these lesions was marked by large numbers of heterophils. The fibrous tissue

extended into the epiphysis and usually obliterated the epiphyseal cartilage. A generalized description of the lesions was that of a large area of heterophile and necrotic debris mixed with large bacterial colonies and lyzed portions of bone trabeculae.

All rabbits were reported to be in good body condition and only four rabbits were reported with pathological lesions in the viscera. These pathological abnormalities were described as follows: (1) One rabbit was reported with a hepatic microabscess, (2) Two rabbits demonstrated thrombosis of several hepatic portal vessels along with large areas of coagulation necrosis with focal hemorrhages and exudations of heterophils. Bile duct proliferation was present in the infected portal triads along with a heavy layer of immature fibroblastic tissue on the hepatic capsule. (3) The kidney of one rabbit presented with large aggregations of lymphocytes and plasma cells beneath the pelvic epithelium and was well walled off by immature fibrous tissue in the renal papilla. One large area of coagulation necrosis was visible in this portion of kidney. The upper tunicia propria of the bladder wall demonstrated focal epithelial sloughing and heavy lymphocytic and plasma cell exudation.

Bacteriological samples were taken from each leg to confirm that Staphylococcus aureus was the causative microorganism and to confirm that the osteomyelitis was not due to a secondary infection caused by some other pathogenic organism. These samples were phage-typed by Dr. A.W. Jackson, Chief, Reference Service, Bureau of Bacteriological Diseases, Canadian Staphylococcus Phage Typing Reference Centre, Laboratory Centre for Disease Control, Health Protection Branch, Health and Welfare Canada, Ottawa, Ontario. These tests confirmed that the

bacteria isolated was Staphylococcus aureus of the same phage type (phage type 47) as that originally used to inoculate the experimental tibiae of the rabbits. No other phage type or pathological organism could be isolated from these animals upon post mortem examination.

Based upon the various approaches to establishment of an osteomyelitis animal model it was found that the rabbit model injected with sclerosing agent and bacteria was the most successful procedure.

C. COMPARISON OF SCINTIGRAPHIC AND RADIOGRAPHIC METHODS FOR DETECTION OF OSTEOMYELITIS

The radiologists and nuclear medicine physicians of the Cross Cancer Institute, Edmonton, Alberta kindly examined and interpreted the five series of animal radiographs and scintiscans presented to them in a double blind technique. The scans and X-rays supplied to them had all identifying information obliterated except the random code number so that they could not identify from the coded radiograph or scintiscan which animal or which day of the experiment they were evaluating. The evaluated data was then decoded, assembled, and presented in Figures I, II, III, IV, and V.

The majority of the individual evaluations required the radiologists to declare whether the radiographs were negative or positive for trauma or osteomyelitis and the scintigraphs normal or abnormal. A symmetrical scintiscan was regarded as normal while asymmetrical uptake of the bone-seeking radiopharmaceutical was evaluated as abnormal. In the event of a no-majority decision, the data was again evaluated by the physicians and a decision was reached by debate.

A series of five experiments was performed to evaluate this rabbit model for osteomyelitis by comparing radiographic and scintigraphic methods. These five experiments and the preliminary work preceding them make up the major part of this thesis project. Different strains of Staphylococcus aureus in different concentrations were tested and evaluated as well as different types and sizes of needles used to introduce the inoculating suspension into the medullary cavity of the rabbit tibia. Preliminary work included the use of several small groups of rabbits to ensure this model of osteomyelitis could be reproduced successfully with a minimum of bone trauma. Undesirable excessive physical insult associated with improper insertion of the inoculating needle could potentially obscure the early, minute signs characteristic of osteomyelitis and perhaps prejudice the interpreting physicians' evaluation of each radiograph.

All the radiographs done in the preliminary experiments and in experimental series 1 and 2 were produced at The Surgical Medical Research Institute, University of Alberta, Edmonton, Alberta where difficulties existed in obtaining good quality radiographs of the limbs of an animal as small as a young rabbit. While careful evaluation of all the results to this point in the series of experiments led to the conclusion that the bone scan was far superior to the radiograph in detecting osteomyelitis, the author was not satisfied that this finding was entirely objective. The experiments were, therefore, repeated with improved radiographic quality.

For the purposes of these experiments, a radiograph was declared to be positive for osteomyelitis if a majority of physicians evaluating the

radiograph judged that signs indicative of the disease process were present. Similarly, a scintiphoto was evaluated to be abnormal if asymmetrical uptake of bone-seeking radiopharmaceutical was seen in the tibiae. For the purposes of analysis of this data, a bone was declared positive for osteomyelitis if radiological concensus was that the radiographs of any given rabbit showed signs indicative of the disease process on two consecutive days or if the scintiphotos of the animal were judged to show asymmetrical uptake for two consecutive days. One of the radiologists at the Cross Cancer Institute who evaluated all of the rabbit roentgenographs stated "the typical rabbit osteomyelitis is characterized by lytic lesions without much proliferative bone formation".

In all five experiments control radiographs and scintiscans of all animals were obtained the day before inoculation and in all cases the radiographs and scintiscans were evaluated as normal.

Experiment 1 (Figure I) is the first experiment of this series. These radiographs were kindly produced by The Surgical Medical Research Institute, University of Alberta, Edmonton but the quality of these radiographs was such that the inoculation site, minute anatomical structures such as the foramina of the bone, and subtle changes indicative of osteomyelitis such as the elevation of the periosteum off the surface of the bone were not visualized. Abnormal scintigraphic findings preceded radiographic changes indicative of osteomyelitis in rabbits 1, 3 and 6 by two days and in rabbits 2 and 7 by 4 days. Rabbits 4 and 5 did not develop osteomyelitis as defined earlier and rabbit 8 died on day 3 before any changes were seen. Observed changes occurred only in the right tibiae because the left bone was not used as

FIGURE I

Summary of evaluations of bone scintiscans and radiographs of experiment Nº 1

Data is presented in units of pairs.

The left member of each pair represents the left tibia while the right member describes the right tibia for any given day.

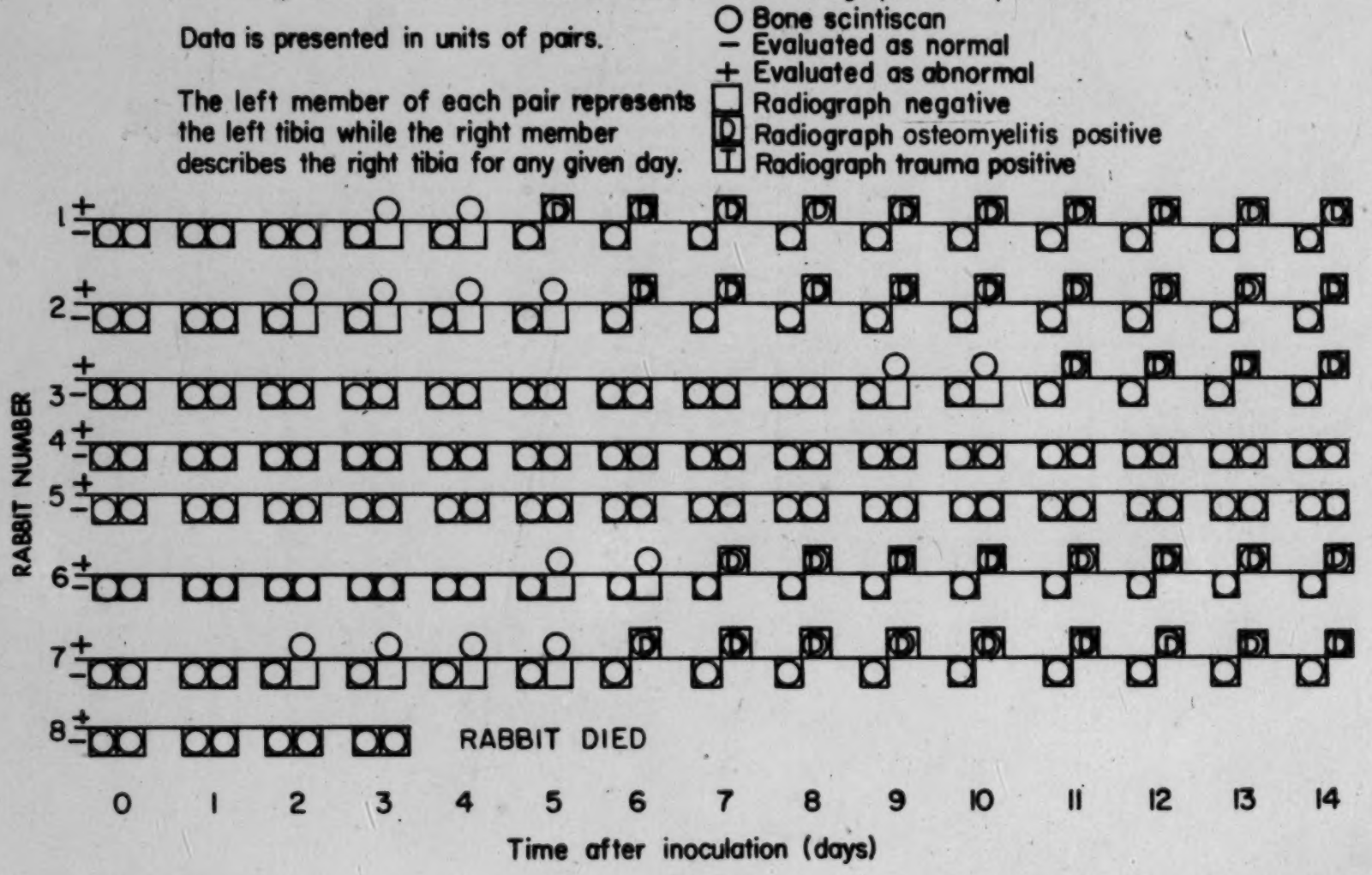

a control - the left tibiae were not subjected to any manipulation or trauma in that a needle was never introduced into the medullary cavity of the left bone to simulate any insult to the tissue which might occur in the right bone upon inoculation.

Experiment 2 (Figure II) incorporated the use of the left tibia as a control bone and the right tibia as the experimental bone. Rabbit 1 showed, perhaps, the most clear-cut differences between radiographic and scintigraphic techniques in that it developed a hematogenous site of osteomyelitis. Photographic plates 1 and 2 illustrate the radiographic and corresponding scintigram of the hematogenous lesion while photographic plates 3 and 4 illustrate a typical radiograph and scintigram seen in a well established case of osteomyelitis following inoculation. The arrows indicate the affected site. The scan findings here preceded the radiographic signs by seven days (day 12 vs day 19) while the right tibia did not develop osteomyelitis.

In all these experiments the protocol was followed for more than 14 days but this was the only lesion that became positive as evaluated by either diagnostic mode beyond 14 days after inoculation. Rabbits 2 and 4 did not develop the signs of disease during the period of observation. Rabbit 3 showed signs of osteomyelitis on the radiograph and an abnormal scintiscan simultaneously on day 11 after inoculation. Rabbit 5 showed signs of disease by scan and radiograph both on day 4. Rabbits 6 and 7 showed scintigraphic changes in day 4 and radiographically on day 6. Rabbit 8 showed scan changes preceding radiographic signs by six days (day 5 vs day 11).

In this series of animals, four rabbits showed that the scan detected osteomyelitis before the radiograph. Two animals demonstrated

FIGURE II

Summary of evaluation of bone scintiscans and radiographs of experiment № 2

Data is presented in units of pairs.

The left member of each pair represents the left tibia while the right member describes the right tibia for any given day.

○ Bone scintiscan
− Evaluated as normal
+ Evaluated as abnormal
□ Radiograph negative
D Radiograph osteomyelitis positive
T Radiograph trauma positive

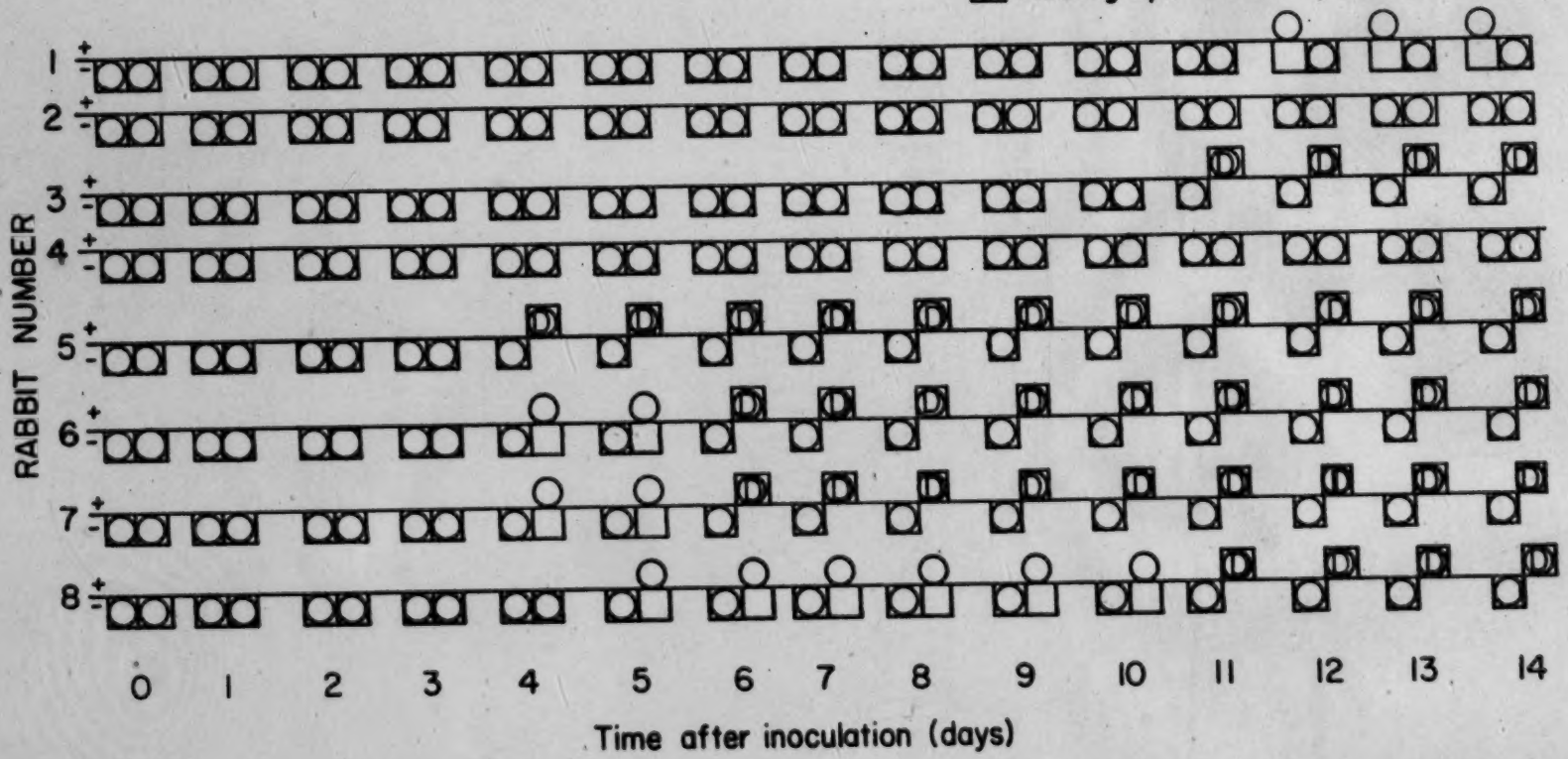

Photographic plate 1. Radiograph of hind limbs of a rabbit with hematogenous osteomyelitis.

Photographic plate 2: Scintigram (Tc-99m-MDP) of hind limbs of a rabbit with hematogenous osteomyelitis. (Corresponding to Radiograph plate 1.)

Photographic plate 3. Radiograph of hind limbs of a rabbit displaying gross osteomyelytic lesions.

Photographic plate 4. Scintigram (Tc-99m-MDP) of hind limbs of a rabbit with advanced osteomyelytic lesions. (Corresponding to Radiographic plate 3.)

simultaneous changes and two animals apparently did not contract the disease. Rabbit 1 demonstrated an extremely rare finding - a hematogenous site of osteomyelitis, which according to reported literature (Wi27, Sc41) is so extremely rare as not to represent a viable experimental method. The left tibiae in experiment 2 and all subsequent experiments were used as control bones in that saline and sodium morrhuate were injected into the medullary cavity of these bones to simulate the experimental procedure in the right tibiae.

In experiments 1 and 2, no histopathological examinations were performed on the animals after termination of the experiments because the quality of the radiographs was such that only gross changes of bone architecture due to disease could be seen. Alterations of the structure of the tibiae appeared so gross as the disease took its course that pathological examinations were not conducted. After evaluation of the cumulative results of the preliminary data and experiments 1 and 2, a decision was made to modify existing radiographic equipment in The Division of Bionucleonics and Radiopharmacy, Faculty of Pharmacy, University of Alberta, Edmonton and develop new techniques to produce high quality roentgenographs to match the quality of clinically-produced radiographs. Further series of experiments were conducted and satisfactory radiographs were produced using the modified equipment and newly developed techniques. Moreover, histopathological examinations were performed on all animals in experiments 3, 4 and 5 to determine more precisely the physical condition of the experimental animals upon termination of the experiments. These histopathological reports were used as the

ultimate standard as to the actual condition of these animals and to which the radiological and scintigraphic data were compared.

A false-positive evaluation is a diagnosis incorrectly interpreted as being positive for osteomyelitis, in these experiments, when histopathological results are negative for signs of the disease. A false-negative evaluation is a judgement incorrectly interpreted as negative for signs of the disease when histopathological results are positive. A true-positive evaluation is one in which the interpretation is positive for signs of disease and the histopathological results are also positive. A true-negative evaluation is one in which the interpretation is negative for signs of osteomyelitis and the histopathological results are also negative.

Experiment 3

Rabbits 1, 2, 3, and 4 showed radiographic changes of osteomyelitis (Figure III) while the corresponding scintiscans showed no such abnormalities. Rabbit 4 demonstrated an interesting phenomenon in that the radiographic evaluations changed back and forth from trauma to disease from day 1 to day 8 and then for the rest of the experiment was judged to be normal in appearance. This phenomenon probably illustrates that the early osseous changes seen by the radiologists are so small that the evaluations of whether they are due to trauma or disease are very subjective. The scan findings of rabbit 5 were judged to be abnormal on day 1 while the radiographic changes characteristic of osteomyelitis were noted on day 4. The bone scan of rabbit 6 was evaluated as abnormal on day 2 while the radiograph was said to be positive for osteomyelitis on day 4. The bone scan and radiograph of rabbit 7 were judged to be characteristic for osteomyelitis

FIGURE III

Summary of evaluation of bone scintiscans and radiographs of experiment Nº 3

Data is presented in units of pairs.

The left member of each pair represents the left tibia while the right member describes the right tibia for any given day.

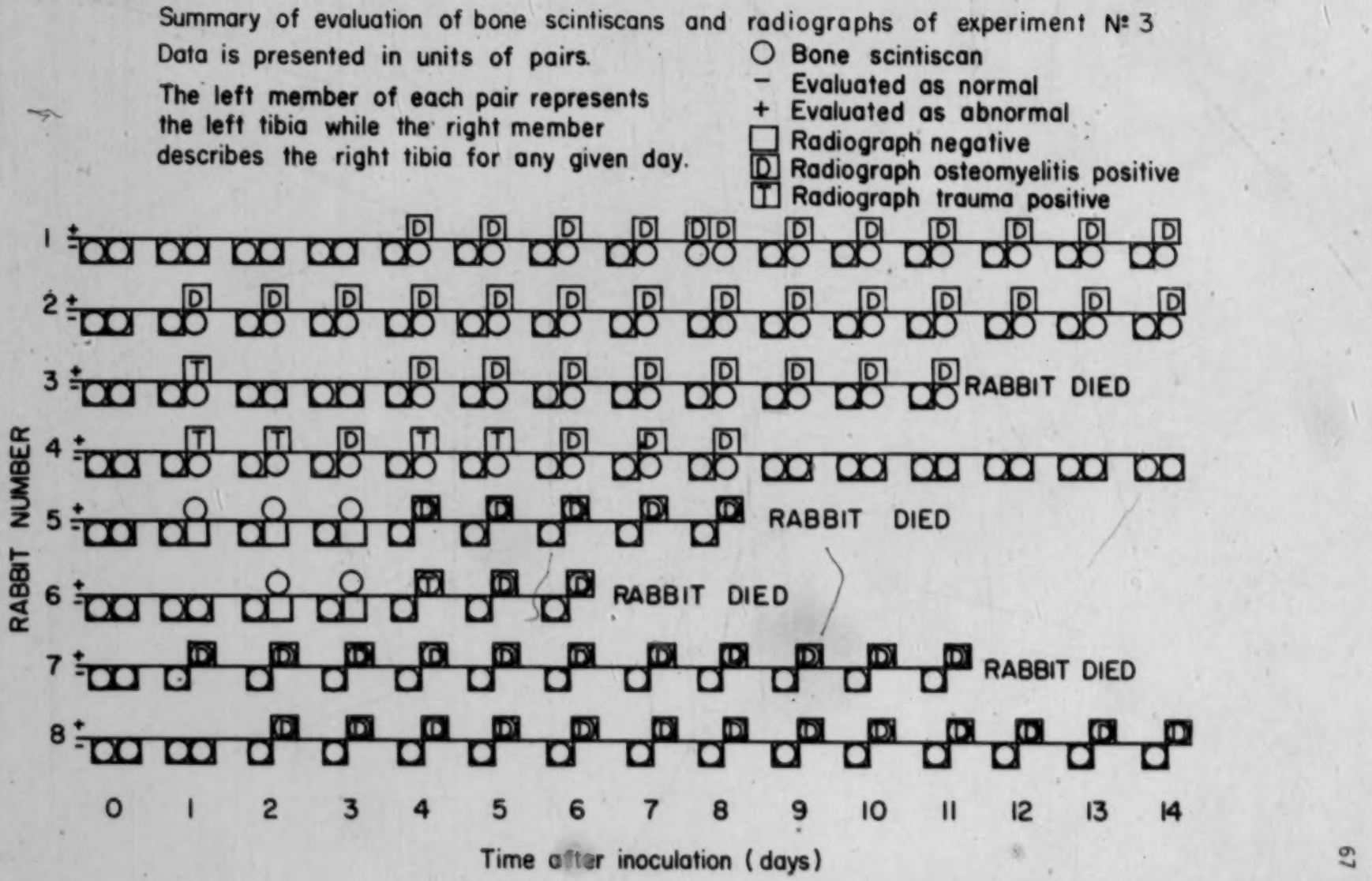

simultaneously on day 1 after inoculation and that of rabbit 8 were also simultaneously characteristic of the disease process on day 2. Histopathological examinations of the rabbits confirmed osteomyelitis in the right limbs of all animals except that of rabbit 3 which was found to be normal. Samples taken from rabbit 7 were cultured and confirmed to contain Staphylococcus aureus. In summary, seven of the eight rabbits were confirmed to have osteomyelitis by histopathological standards. Two of these were detected simultaneously by bone scan and radiographic technique. Three rabbits demonstrated changes by radiographic techniques and not scintigraphic procedures. Scintiscans showed false-negative positive results by radiographic interpretation while scintigraphic methods produced true-negative findings as confirmed by tissue examination.

Experiment 4

Radiographic data for rabbit 1 first showed signs of osteomyelitis on day 3 but the first two such consecutive findings occurred on days 7 and 8 when both tibiae showed signs which the radiologists interpreted as positive (Figure IV). The scintiscan of the right tibia was not interpreted as abnormal during this experiment while that of the left tibia was positive only on day 1, soon after the traumatic effects of inoculation.

The radiographic findings for the left tibia of rabbit 2 showed it to be positive for osteomyelitis on day 6 while the right leg was judged positive on day 10. The scintiscan of the right tibia was not judged abnormal during the experiment while the left was abnormal only on days 3 and 8.

FIGURE IV

Summary of evaluation of bone scintiscans and radiographs of experiment Nº 4

Data is presented in units of pairs.

The left member of each pair represents the left tibia while the right member describes the right tibia for any given day.

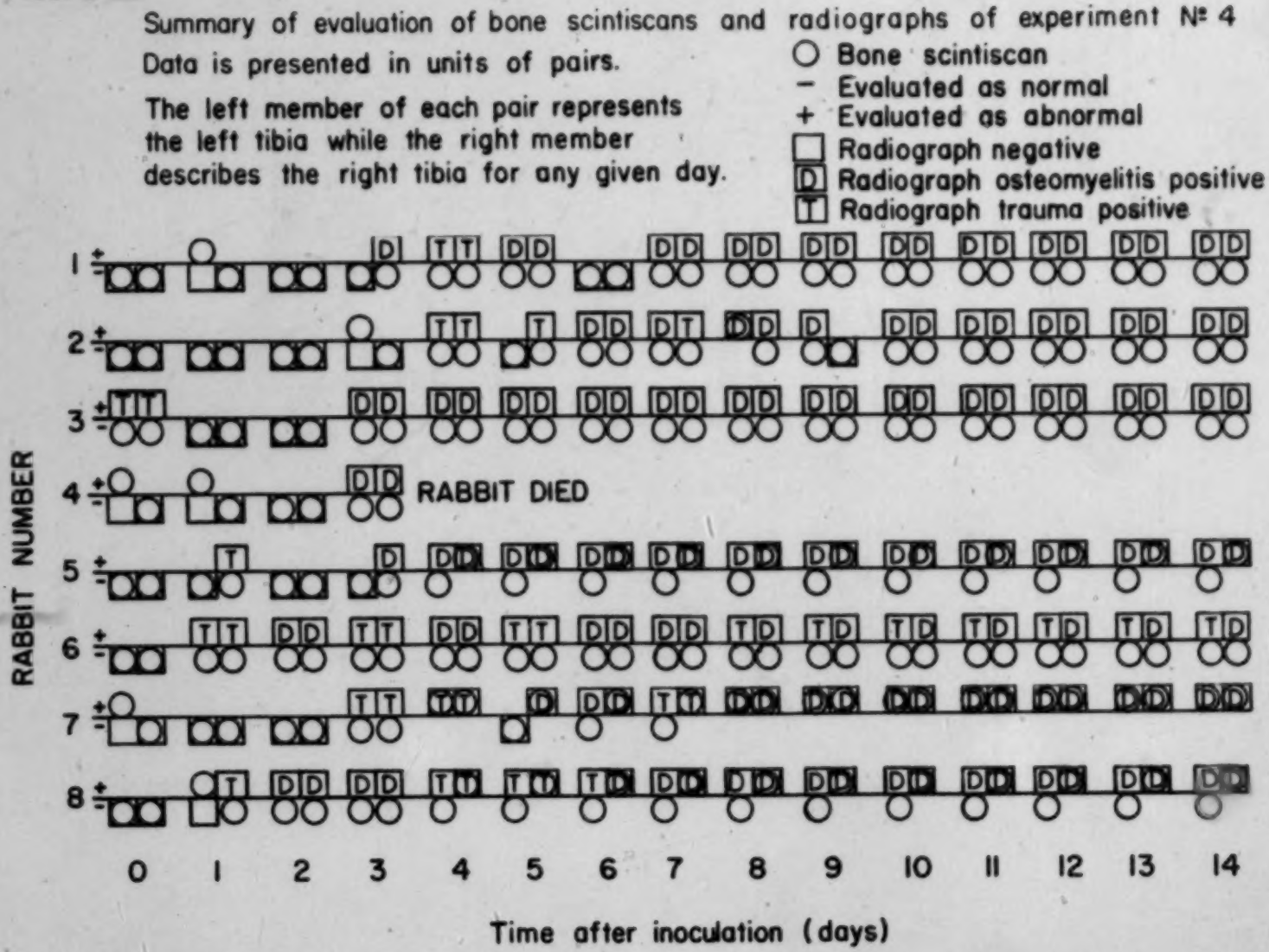

The scintigraphic findings for rabbit 3 were consistently normal while radiographic results for both tibiae were simultaneously positive on day 3. Scintigraphic results on rabbit 4 showed abnormal uptake on days 0 and 1 in the left leg while showing positive radiographic signs of osteomyelitis only on day 3 on which it died.

Radiographic evaluations were positive for osteomyelitis for rabbit 5 for the right leg from days 3 to 14 and the left leg from days 4 to 14. The scintiscan of the left leg was consistently reported as negative while the right leg was reported as abnormal from days 4 to 14.

Radiographic evaluations for rabbit 6 showed that interpretations for the left leg changed often from traumatic to osteomyelitis positive but ended with seven consecutive evaluations of trauma while the right tibia was judged to be positive for osteomyelitis as of day 6. Scintigraphic findings were always reported as normal.

Scintigraphic and radiographic data for the right tibia of rabbit 7 were evaluated as positive simultaneously as of day 5 and for the left leg simultaneously as of day 8.

Radiographic data for rabbit 8 showed the right and left tibiae to be positive for osteomyelitis as of day 2 while the scintigraphic data showed the left tibia to be consistently reported as normal while the right tibia was reported as abnormal from days 4 to 14.

The histopathological review of these animals was done at day 17 of this experiment and a summary of this report is as follows: "The lesions noted in the tibiae of all these rabbits are very similar. The left tibia of each rabbit #1-#8 demonstrates similar changes. There is a severe necrotizing reaction immediately beneath the epiphyseal plate. A large area of necrosis demonstrates numerous large bacterial colonies

consisting of cocci. Lysis of bone is a predominant feature and surrounding these areas of necrosis there is a fibrous tissue proliferation. Large numbers of heterophils are present on the periphery of these lesions. The fibrous tissue reaction extends into the epiphysis and in most cases obliterates the epiphyseal cartilage. Large areas of necrotic debris and heterophils are mixed with lyzed portions of bony trabeculae and large bacterial colonies. A similar necrotizing reaction is present in the right tibia of rabbits #1, #3, #4, #6, #7, and #8 there are a few bacterial colonies but not nearly as prominant nor as large as in the left tibia of these rabbits. In rabbits #2 and #5 no bacteria are present although there was a moderate necrotizing reaction to the injection."

In summary, radiographic results for rabbit 1 were 2 true positive findings while scintigraphic evaluations produced 2 false negative findings.

The roentgenographic results of rabbit 2 produced 1 true and 1 false positive finding while radiographic methods provided 1 false negative and 1 true negative evaluation.

Two true positive findings were obtained by radiographic methods on rabbit 3 while scintigraphy provided 2 false negative results.

Radiography produced 1 false negative finding on rabbit 4 while scintigraphy produced 1 true positive result.

One false positive and 1 true positive result were produced by radiographic evaluation of rabbit 5 while 1 false positive and 1 false negative resulted from scintigraphic methodology.

Radiography provided 1 false negative and 1 true positive finding on rabbit 6 while 2 false negative resulted from scintigraphic analysis of the data available for rabbit 6.

Radiography produced 2 true positive findings for rabbit 7 as did scintigraphy with the lesion in the right tibia being detected simultaneously by both methods while radiographic evaluation of osteomyelitis in the left tibia preceded that by scintigraphy by 5 days.

Two true positive evaluations were produced by radiographic evaluation in rabbit 8 with 1 false negative and 1 true positive finding by scintigraphic methods. The lesion in the right leg was determined simultaneously by both methods.

Experiment 5

Rabbits 1 and 2 of this experiment were controls which were injected only with saline and sodium morrhuate but no bacteria. No bacteria could be cultured from these animals and no lesions were reported in the legs of these animals similar to those of any other rabbits submitted for histopathological examination.

In this experiment the histopathological report was regarded as representing the true physical condition of the animal and the radiographic and scintigraphic evaluations were compared to the autopsy report. A true negative result was one in which both the radiograph or scintiphoto were evaluated as negative as well as the histopathological report. A true positive result was a radiograph or scintigraph seen as positive for the disease process as well as the tissue examination. A false negative result was a roentgenograph or scintiscan judged to be normal while the histopathological report stated presence of osteomyelitis. A false positive evaluation was a radiograph or

scintiimage judged to show signs of disease accompanied by a tissue examination reported as being normal.

Osteomyelitis in the right tibia was diagnosed radiographically in rabbit 3 on day 6 (Figure V) and the left leg was consistently evaluated as normal while the bone scans showed both legs to be normal during the experiment. The histopathological report was abscess with fibrosis in the right tibia with no visible lesion in the left. Thus the radiographic method showed a true positive and a true negative judgment while the scintiscan showed one true negative and one false negative evaluation.

Radiographic data for rabbit 4 showed both tibiae to be positive as of day 2. Scintigraphic data showed the left tibia to be normal while the right tibia was judged to be abnormal from day 5. The histopathological report for rabbit 4 was slight sclerosis in the left tibia with a diaphyseal abscess and metaphyseal infarction in the right bone. Radiography produced one true positive and one false positive evaluation while scintigraphy produced one true negative and one true positive.

The radiographic technique showed disease consistently in rabbit 5 from day 3 to 14 in both tibiae while the scintiscan showed disease only in the right tibia and only from day 4 to 14. The autopsy of this animal showed a large abscess containing bacteria in the right leg with no sample available for the left. The radiographic methods showed one true positive and scintigraphy one true positive result.

Radiographic data showed both tibiae of rabbit 6 positive from day 3 while scintigraphic data were always normal for both bones. The tissue samples from rabbit 6 showed a large abscess in the left tibia

FIGURE V

Summary of evaluation of bone scintiscans and radiographs of experiment Nº 5

Data is presented in units of pairs

The left member of each pair represents the left tibia while the right member describes the right tibia for any given day.

○ Bone scintiscan
− Evaluated as normal
\+ Evaluated as abnormal
□ Radiograph negative
[D] Radiograph osteomyelitis positive
[T] Radiograph trauma positive

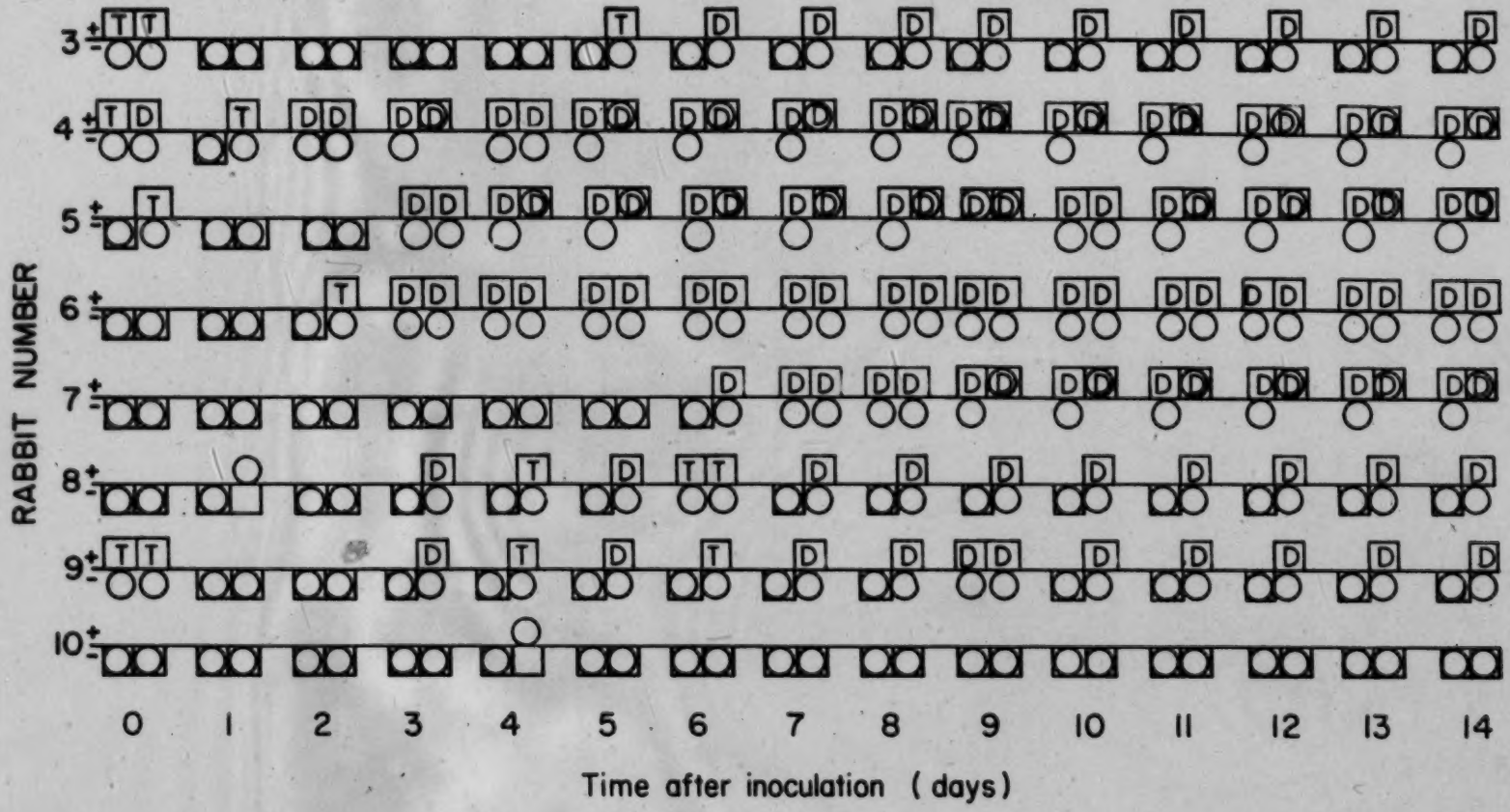

and nondefinable results from the right bone. Thus radiographic techniques produced one true positive while scintigraphic methods produced one false negative result.

Radiographic methods showed positive results in the right leg of rabbit 7 from day 6 while scintigraphic methods showed positive data from day 9. The left leg was judged positive by roentgenographic methods on day 7 while the bone scan always showed normal distribution of the radiotracer. The tissue samples from rabbit 7 showed abscess in the right leg with only some sclerosis present in the left tibia. Radiographic methodology produced one true positive and one false positive result while scintigraphic techniques produced one true positive and one true negative result.

The right tibia of rabbit 8 was evaluated by radiographic methods to show signs of disease from day 7 with the left leg remaining normal while the bone scans were evaluated consistently as normal except for the right tibia on day 1 (soon after the traumatic procedure of inoculation). Histopathological results from rabbit 8 showed no lesion in the right tibia with samples from the left tibia showing no signs of active osteomyelitis. Radiographic data showed one false positive and one true negative while scintigraphic data showed two true negative results.

Radiographic data from rabbit 9 showed the right tibia to be positive from day 7 while the left bone was always interpreted as normal. Scintigraphic data for both tibiae were always seen as normal. Autopsy results showed no signs of osteomyelitis in either tibia. Radiographic results showed on true negative and one false positive lesion. Scintigraphic results showed two true negative interpretations.

All scintigraphic data from rabbit 10 was judged to be negative. The scintigraphic data was consistently evaluated as showing normal uptake of radiotracer except for the single exception of the right tibia on day 4. Histopathological results for rabbit 10 reported slight sclerosis of the right tibia with no visible lesion of the left bone. Radiographic procedures produced two true negative results as did scintigraphic methods.

D. ANALYSIS OF RADIOGRAPHIC AND SCINTIGRAPHIC DATA

For the purposes of analysis of these 5 experiments the data were divided into 2 groups - the first group composed of the data from experiments 1 and 2 in which no histopathological data was available and only gross anatomical changes could be seen because of the poorer quality of the radiographs available and the second group composed of the data from experiments 3, 4, and 5 in which histopathological results were available as well as good quality radiographs.

1. Analysis of Data from Experiments 1 and 2

The reduced data from experiments 1 and 2 is presented in Tables 4 and 5. Column 1 presents the rabbit number; column 2 presents the leg evaluated; column 3 presents the presence or absence of disease as evaluated by radiographic or scintigraphic interpretation; column 4 presents the diagnostic methodology which first showed positive signs for osteomyelitis; and column 5 presents the number of days between positive evaluation of indicative signs for osteomyelitis, if such a difference exists. Eleven positive diagnoses for osteomyelitis were obtained in 16 animals in experiments 1 and 2. Two of these diagnoses were seen simultaneously by both radiography and scintigraphy while 9

TABLE 4

Data Reduction of Experiment 1

Rabbit #	Leg	Presence of Osteomyelitis	First Method to Detect Osteomyelitis	Time Advantage (Days)
1	Left	-	-	-
	Right	+	Scintigraphy	2
2	Left	-	-	-
	Right	+	Scintigraphy	4
3	Left	-	-	-
	Right	+	Scintigraphy	2
4	Left	-	-	-
	Right	-	-	-
5	Left	-	-	-
	Right	-	-	-
6	Left	-	-	-
	Right	+	Scintigraphy	2
7	Left	-	-	-
	Right	+	Scintigraphy	4
8	Left	Died	-	-
	Right		-	-

+ = Positive evaluation for osteomyelitis by radiography or scintigraphy

- = No signs of osteomyelitis as evaluated by radiography or scintigraphy

TABLE 5

Data Reduction of Experiment 2

Rabbit #	Leg	Presence of Osteomyelitis	First Method to Detect Osteomyelitis	Time Advantage (Days)
1	Left	+	Scintigraphy	7
	Right	-	-	-
2	Left	-	-	-
	Right	-	-	-
3	Left	-	-	-
	Right	+	Simultaneous	-
4	Left	-	-	-
	Right	-	-	-
5	Left	-	-	-
	Right	+	Simultaneous	-
6	Left	-	-	-
	Right	+	Scintigraphy	2
7	Left	-	-	-
	Right	+	Scintigraphy	2
8	Left	-	-	-
	Right	+	Scintigraphy	6

+ = Positive evaluation for osteomyelitis by radiography or scintigraphy

- = No signs of osteomyelitis as evaluated by radiography or scintigraphy

were first detected using scintigraphic methods. The number of days between positive evaluation of signs of osteomyelitis in these 9 animals ranged from 2 to 6 with a mean value of 3.4 days and a standard deviation of 1.9 days.

Tables 6, 7, and 8 present the data obtained from experiments 3, 4, and 5 respectively in the same manner as in Tables 4 and 5. This data from Tables 6, 7, and 8 is further reduced and presented in Table 9. Differences between group 1, the data assembled from experiments 1 and 2, and from group 2, the data from experiments 3, 4 and 5 are notable.

In group 1, 11 positive evaluations for osteomyelitis were obtained from 16 animals. The observed changes in bone structure were gross enough to be detected by the poorer quality radiographs first produced. Two of these 11 lesions were observed simultaneously by scintigraphic and radiographic methods while the other 9 lesions were all first detected by the scintigraphic method. Scintiscanning offers an advantage over radiographic methods for successful diagnosis of early signs positive for osteomyelitis. Similar results to these have been reported in the literature where human clinical studies have been presented in which scintiscanning methodology has been shows to precede radiographic signs indicative of osteomyelitis by at least several days (Tr76, Ha76, Ru76, Ca70, Gi75, Du75, Ma76, Ge77, Li77). Other workers (Tr76, Ch64) have reported that 30-50% of bone mineral must be removed before a lytic bone lesion will be visible on a radiograph, also indicating that gross changes in bone are being used as radiological signs of osteomyelitis. The experimental data from group 1 agrees well with these reports in the literature.

2. Analysis of Data from Experiment 3, 4, and 5

Group 2, consisting of experiments 3, 4, and 5 used the histopathological reports to represent the actual physical condition of the animals at the end of each experiment to which the radiographic and scintigraphic evaluations were compared. The diagnostic interpretations were divided into four groups: true negative (T-), true positive (T+), false negative (F-), and false positive (F+) by the following criteria:

T- = Histopathological report is negative:
Diagnostic evaluation is negative

T+ = Histopathological report is positive:
Diagnostic evaluation is positive

F- = Histopathological report is positive:
Diagnostic evaluation is negative

F+ = Histopathological report is negative:
Diagnostic evaulation is positive

The results of experiments 3, 4, and 5 appear in Tables 6, 7, and 8. Of the 9 true positive lesions detected by both radiographic and scintigraphic methods in 24 animals 2 were detected simultaneously by both radiographic and scintigraphic methods; scintigraphy detected 3 lesions before radiography by 1, 2, and 3 days respectively while diagnostic radiography detected 4 before scintigraphic evaluations did by 1, 2, 3, and 5 days respectively.

TABLE 6

Data Reduction of Experiment 3

Rabbit #	Leg	Radiographic Findings	Scintigraphic Findings	First Method to Detect Osteomyelitis	Time Advantage (Days)
1	Left	T-	T-	-	-
	Right	T+	F-	Radiography	-
2	Left	T-	T-	-	-
	Right	T+	F-	Radiography	-
3	Left	T-	T-	-	-
	Right	F+	T-	-	-
4	Left	T-	T-	-	-
	Right	T+	F-	Radiography	-
5	Left	T-	T-	-	-
	Right	T+	T+	Scintigraphy	3
6	Left	T-	T-	-	-
	Right	T+	T+	Scintigraphy	2
7	Left	T-	T-	-	-
	Right	T+	T+	Simultaneous	-
8	Left	T-	T-	-	-
	Right	T+	T+	Simultaneous	-

T- = True negative: Histopathological report = negative: Diagnostic evaluation = negative

T+ = True positive: Histopathological report = positive: Diagnostic evaluation = positive

F- = False negative: Histopathological report = positive: Diagnostic evaluation = negative

F+ = False positive: Histopathological report = negative: Diagnostic evaluation = positive

TABLE 7

Data Reduction of Experiment 4

Rabbit #	Leg	Radiographic Findings	Scintigraphic Findings	First Method to Detect Osteomyelitis	Time Advantage (Days)
1	Left	T+	F-	-	-
	Right	T+	F-	-	-
2	Left	T+	F-	-	-
	Right	F+	T-	-	-
3	Left	T+	F-	-	-
	Right	T+	F-	-	-
4	Left	F-	T+	-	-
	Right	F-	F-	-	-
5	Left	F+	F+	-	-
	Right	T+	F-	-	-
6	Left	T+	F-	-	-
	Right	F-	F-	-	-
7	Left	T+	T+	Radiography	5
	Right	T+	T+	Scintigraphy	1
8	Left	T+	F-	-	-
	Right	T+	T+	Radiography	2

T- = True negative: Histopathological report = negative: Diagnostic evaluation = negative

T+ = True positive: Histopathological report = positive: Diagnostic evaluation = positive

F- = False negative: Histopathological report = positive: Diagnostic evaluation = negative

F+ = False positive: Histopathological report = negative: Diagnostic evaluation = positive

TABLE 8

Data Reduction of Experiment 5

Rabbit #	Leg	Radiographic Findings	Scintigraphic Findings	First method to Detect Osteomyelitis	Time Advantage (Days)
3	Left	T-	T-	-	-
	Right	T+	F-	-	-
4	Left	T+	T+	-	-
	Right	F+	T-	-	-
5	Left	(No sample available)		-	-
	Right	T+	T+	Radiography	1
6	Left	T+	F-	-	-
	Right	(Nondefinable histopathological results)		-	-
7	Left	F+	T-	-	-
	Right	T+	T+	Radiography	3
8	Left	T-	T-	-	-
	Right	F+	T-	-	-
9	Left	T-	T-	-	-
	Right	F+	T-	-	-
10	Left	T-	T-	-	-
	Right	T-	T-	-	-

T- = True negative: Histopathological report = negative: Diagnostic evaluation = negative

T+ = True positive: Histopathological report = positive: Diagnostic evaluation = positive

F- = False negative: Histopathological report = positive: Diagnostic evaluation = negative

F+ = False positive: Histopathological report = negative: Diagnostic evaluation = positive

TABLE 9

SUMMARY OF RADIOGRAPHIC AND SCINTIGRAPHIC EVALUATIONS

Experiment #	# of Definable Tissue Reports	# T-		# T+		# F-		# F+	
		R	S	R	S	R	S	R	S
3	16	8	9	8	4	0	3	0	0
4	16	0	1	11	4	3	10	2	1
5	14	5	9	5	3	0	2	4	0
	46	13	19	24	11	3	15	6	1

R = Radiographic Method

S = Scintigraphic Method

T- = True negative: Histopathological report = negative: Diagnostic evaluation = negative

T+ = True positive: Histopathological report = positive: Diagnostic evaluation = positive

F- = False negative: Histopathological report = positive: Diagnostic evaluation = negative

F+ = False positive: Histopathological report = negative: Diagnostic evaluation = positive

Several authors have evaluated physicians diagnostic decisions involving radiographic images (Th69, Th75, He69, Ye69, Ku75, Ku79, Sq69) and receiver operating - characteristic (ROC) curve (Me76, St75, Sw77, Tu78, Tu78a). A simple type of explanation of this type of analysis is provided by Turner (Tu78a) who described a radiographic or scintigraphic image as a complicated composition where disease ("signals") are found along with "noise", e.g. anatomic structures, artefacts, or normal variations which confuse or mimic signs for which the observer is searching. While strong signals, such as gross anatomical changes, are easily discriminated from background noise, subtle anomalies will be hard to detect. If an observer evaluates an image as positive whenever he sees something he judges to be abnormal, he will produce a large number of false-positive results and will miss very few lesions. "The sensitivity of the test (sensitivity = number of abnormal patients with "positive" tests divided by total number of abnormal patients) will appear to be high but the specificity of the test (specificity = number of normal patients with "negative" tests divided by total number of normal patients) will be low" (p. 435). Specificity can be increased by the observer by evaluating an image as "positive" only when he is certain that the signs of disease are present ("strong signal") but this results in missing the subtle abnormalities and operating with a reduced sensitivity (Tu78a). This model assumes that the observer cannot avoid errors but by adjusting his "criterion level", he can predetermine what error he is likely to make (false negative against false positive) (Tu78a). If one plots a graph of changing sensitivity against specificity as the criterion level is changed, a smooth curve will be

produced known as the receiver-operating-characteristic (ROC) curve (Tu78a). Turner reported that this ROC model accounts for the greatest amount of inter- and intra- observer variation as long as the observers agree as to which signs are potentially abnormal (Tu78a). Turner further reported that observers do not hold their criterion levels constant and most often evaluate an image as positive if other clinical data implies disease is present and further states that "we can expect observer behavior in clinical practice to be characterized by fluctuating sensitivity and specificity" (p. 436) (Tu78a).

The true positive, true negative, false positive, and false negative fraction calculations are shown in Table 10. Radiography showed a sensitivity of 0.89 with a specificity of 0.68 while scintigraphy demonstrated a sensitivity of 0.42 and a specificity of 0.95. These radiographic results showing a high sensitivity and low specificity are characteristic of a "lax" criterion level (Tu78) while the combination of a high specificity and low sensitivity shown with radiographic analysis are produced by a "strict" criterion level (Tu78). Many of the lesions were described as juxta epiphyseal and any increased activity delineating the lesion may be masked by that at the growing end (Gu80). If these lesions were located away from these growing regions which are normally "hot" so that visualization would be possible, more true positive and fewer false negative evaluations might be made which would then result in greater sensitivity without affecting specificity. Three possible reasons exist for the "lax" criterion associated with the radiographic evaluations: (1) the signs characteristic of this rabbit

TABLE 10

Final Data Reduction of Experiments 3, 4, and 5

		Radiography	Scintigraphy
True Positive Fraction	$= \frac{(T+)}{(T+) + (F-)}$ = "Sensitivity"	$\frac{24}{24 + 3} = 0.89$	$\frac{11}{11 + 15} = 0.42$
True Negative Fraction	$= \frac{(T-)}{(T-) + (F+)}$ = "Specificity"	$\frac{13}{13 + 6} = 0.68$	$\frac{19}{19 + 1} = 0.95$
False Positive Fraction	$= \frac{(F+)}{(T-) + (F+)}$ = 1 - (T- Fraction)	$\frac{6}{18 + 6} = 0.25$	$\frac{1}{19 + 1} = 0.05$
False Negative Fraction	$= \frac{F-}{(T+) + (F-)}$ = 1 - (T+ Fraction)	$\frac{3}{24 + 16} = 0.08$	$\frac{15}{11 + 15} = 0.58$

model for osteomyelitis are different from those in the human clinical situation and the physicians evaluating these diagnostic images had to learn the new signs and while doing so were calling any abnormality an osteomyelytic lesion, (2) the physicians knew they were looking only for signs of one disease process while in normal clinical radiographic interpretation any of a large number of diseases or types of trauma which they would have to carefully consider and eliminate to 1 or several only types of lesion, and (3) the physicians were indeed using their criteria for diagnosing osteomyelitis in the human clinical situation on this animal model for osteomyelitis and, in fact, do have "lax criteria" because the "cost" of missing such signs means pain and possibly surgery for the patient as well as health care costs including physicians' time and fees, and hospital and administration costs. Appropriate therapy in the early stages of disease is effective and consists simply of antibiotic drugs which are relatively cheap, provide little inconvenience for the patient, and are easily administered. Even if the diagnosis of osteomyelitis is incorrect, the patient will not be at all impaired by the administration of these drugs. Although the intent of this experimental procedure was not to do any extensive analysis of interobserver variability, 210 paired observations from experiment 4 were examined and disagreement on scintiscans was found to be 7% while disagreement on radiographs was 29%. These figures show that radiographic interpretations are very subjective and that the criterion levels varied between observers more so for the radiographic interpretations than the scintigraphic evaluations. The ROC curve model is reported to account for both inter- and intra- observer variation as

long as the observers agree as to which signs are potentially abnormal (e.g. a "cold" spot in a hepatic scintiscan) (Tu78a).

The data from experiments 3, 4, and 5 do not provide information at all similar to that from experiments 1 and 2 which suggests that if only gross or "classical" symptoms (Ca70) make up the criterion for such experiments, scintiscanning procedures do provide positive diagnosis several days before such data can be obtained from diagnostic radiographs. Cases of classical acute osteomyelitis with negative bone scans have also been reported (Ha76, Ha80, Ga77, Ri77) and Balsam et al. (Ba80) reported a false positive human clinical diagnosis based on a bone scintiscan. Furthermore, Handmaker (Ha80) has reported "hot" and "cold" defects observed in bone scintiscans in clinical cases of human osteomyelitis as well as observing "extended uptake" in which the hypothesis is made that reflex hyperemia is responsible for all adjacent or distal long bones seeming "hot". Sullivan et al. (Su80) have reported that osteomyelitis provides a wide variety of scintigraphic images and presented data from 21 children in which 11 ^{99m}Tc pyrophosphate scintigrams were abnormal, 4 demonstrated subtle changes, and 2 were misleading. Dye et al. (Dy79) showed that the ^{99m}Tc phosphate scan correlated with periosteal new bone in a rabbit model of osteomyelitis in 17 of 18 tibiae while the ^{67}Ga citrate scintiscan correlated with intramedullary alterations and was more sensitive earlier than the ^{99m}Tc phosphate scan. Handmaker (Ha80) also recommended that the radiogallium scintiscan for patients whose ^{99m}Tc phosphate scintiscans provided negative or inconclusive results when infection is suspected. He also reported that the positive ^{67}Ga citrate scintiscan more often shows the true active state of the disease process

than the ^{99m}Tc phosphate scintiscan. Gilday (Gi80) reported that the bone scintigram is "highly inaccurate" in children under 6 weeks of age but much more accurate in patients older than this age group. Ash and Gilday (As80) reported that in 10 neonates (6 weeks of age or less) proven to have osteomyelitis in 20 sites, only 6 sites (31.5%) could be detected by ^{99m}Tc phosphate scintiscans, 58.0% were normal, and 10.5% were equivocal. It is possible that since the rabbits used in the present experiments were of this age group, these bone scintigrams also might not be as good an indicator of osteomyelitis as in older animals.

E. DYNAMIC UPTAKE OF TC-99m MDP IN NORMAL AND INFECTED RABBIT LIMBS

A carrier effect with pyrophosphate and methylene diphosphonate has been reported at injected concentrations of 10 - 500 µg/kg body weight (Su76) and also with the monohydrogen and dihydrogen phosphates but not with the other phosphates and phosphonates (Su76). The levels of methylene diphosphonate in the formulation used in these experiments was 100 µg/kg body weight. Subramanian et al. (Su76) reported rabbit tissue distribution studies showing that within the range of 80-120 µg/kg, maximum skeletal uptake occurred with only minimal liver uptake. This range was also representative of the upper chemical levels used clinically in patients (Su76).

Matched, collimated NaI (Tl) detectors, a multichannel analyzer, and associated electronic equipment were used to perform several kinetic uptake studies on a normal and affected rabbit to compare uptake of ^{99m}Tc-MDP in the right tibiofibular complex and normal contralateral left bone. Fig. VII illustrates the levels of radioactivity throughout a two hour post-injection period as monitored over the rabbit's ear (to

measure blood levels) and over the diseased limb and normal limb. Two distinct portions of the time-activity curve are evident: this is in agreement with the description of Lentle et al. (Le76) who indicated that the initially high radioactivity marked the arrival of the radiopharmaceutical in the vascular system followed later by a progressive extraction of radiopharmaceutical from the blood. In the normal rabbits no significant differences could be seen between the uptake and extraction phase in the right and left limbs in that the uptake curves by the bones from the left and right limb were superimposed over each other, in both the vascular and extraction phases (Fig. VI). However, the rabbit presenting with experimentally induced bone disease produced a different uptake curve for ^{99m}Tc methylene diphosphonate (Fig. VII) in that the vascular phase of the affected bone showed a relatively steeper rise with more accumulation of radiotracer in the first 10 minutes after injection of the radiopharmaceutical than in normal bone. The observed results from this series of experiments would support the findings of Genant et al. (Ge74a) who reported that short term uptake of ^{99m}Tc-EDHP was highly dependent on blood flow and largely independent of the rate of osteogenesis. The experimental data from the present study showed relatively more uptake by the affected bone in the first ten minutes after injection compared to the normal bone, while in healthy rabbits there was no apparent difference in levels of uptake between the two tibiofibular complexes. After approximately 10 minutes following injection of the radiopharmaceutical, the uptake curves of the normal and affected bone appeared to be essentially parallel (Fig. VII).

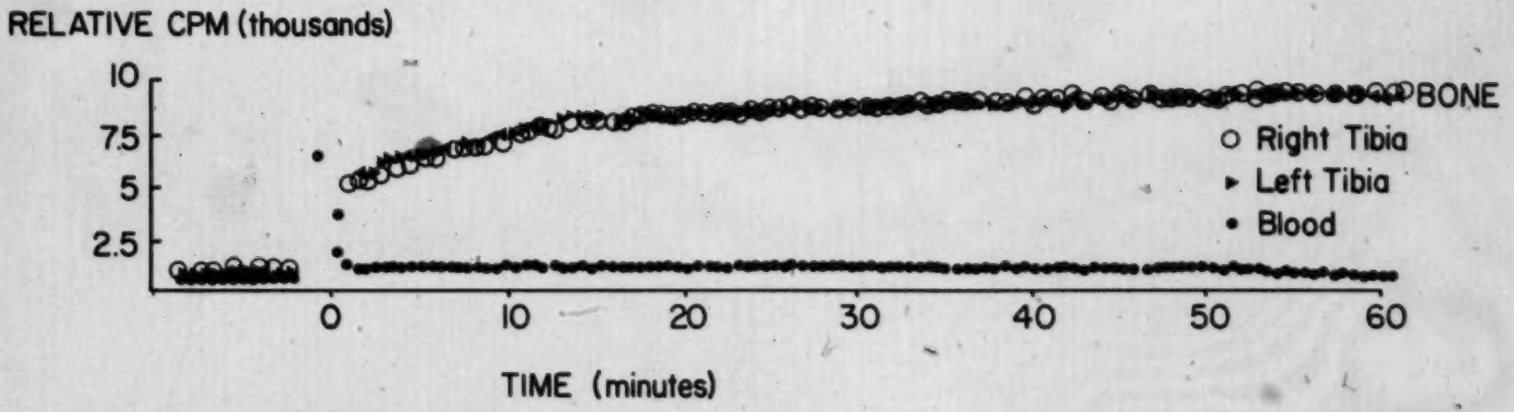

Figure VI Dynamic Uptake of ^{99m}Tc Methylene Diphosphonate in a Normal Rabbit

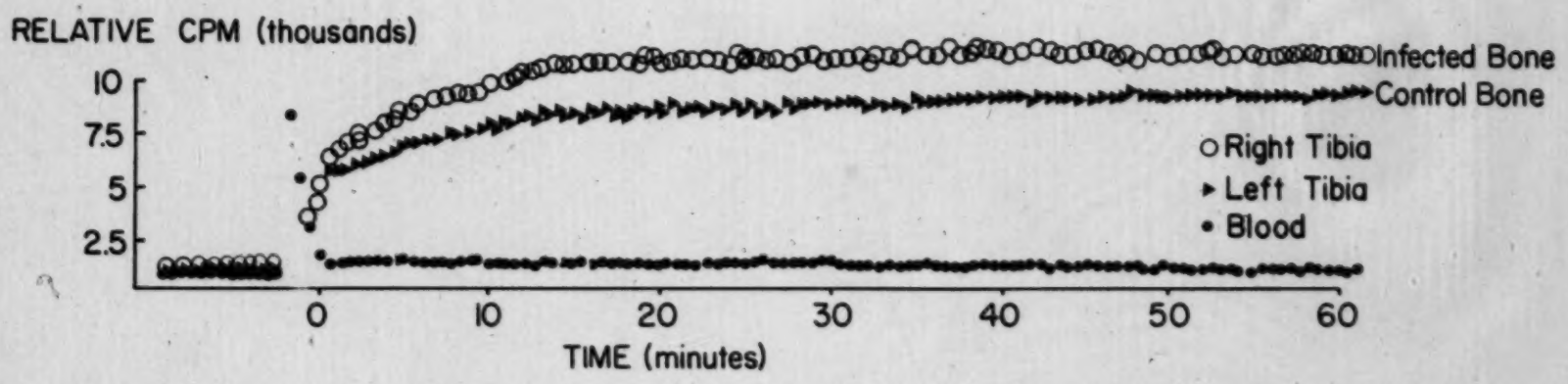

Figure VII Dynamic Uptake of ^{99m}Tc Methylene Diphosphonate in an Osteomyelitis-Positive Rabbit

The uptake curve in Figure VI represents a cumulative curve composed of two distinct elements (Po70): (1) the clearance of the radiopharmaceutical from the blood which showed high levels immediately after intravenous administration and then dropped as the tracer was removed from the blood by (a) becoming associated with the bone (Su75, Fr79, Ge74a, Le76) and (b) by excretion, mainly by the kidney (Su75, Su76); and (2) the actual uptake curve representing association of the ^{99m}Tc-MDP with the bone (Su75, Fr79, Ge74, Le76). The ear was chosen as an appropriate site to monitor blood clearance because there is no bone present which would produce data similar to that obtained from the detector over the rabbit's leg. The collimated detectors over the rabbit's limbs monitored the cumulative bone and blood levels of radioactivity because there was no suitable method of isolating and separating the blood supply, especially the femoral artery from the bone out of the field of view of the detector.

These findings for the rabbit model for osteomyelitis differ somewhat from those reported by Lentle et al. (Le76) which were observed in human Pagetoid bone and in human bone replaced by tumour where differences in uptake of ^{87m}Sr and ^{99m}Tc-polyphosphate were reported in the phase of progressive extraction but not seen in the first 10 minutes immediately following intravenous injection.

F. Static Uptake Studies of ^{99m}Tc Methylene Diphosphonate

Observation of the dynamic uptake experimental data of the rabbit model for osteomyelitis (Fig. VII) shows differences in amounts of localized radioactivity between the unaffected and diseased bones several minutes after intravenous injection of ^{99m}Tc

methylene diphosphonate. A series of studies was devised in which a group of rabbits was inoculated for osteomyelitis with the standard protocol previously described and then intravenously injected with tracer (approximately 80 μ Ci) amounts of ^{99m}Tc MDP. The tibiofibular complexes of each animal were monitored on alternate days over a collimated NaI(Tl) crystal on a shielded platform at 30 and 60 minutes after injection. Then each animal was injected with a scanning dose (700 μCi) of ^{99m}Tc-MDP and imaged with a gamma camera two hours later. Comparative radiographs were also obtained at this time. In order that each animal could serve as its own control, an uptake, scintiscan, and radiogaphic study were done on each animal prior to inoculation.

For the purposes of statistical analysis of the static uptake data, the approach used was to determine the difference in uptake of the radiotracer between the two tibiae which was then related to the sum of the observed radionuclide uptakes in the two bones. The mathematical equations used for the statistical analysis are as follows:

$$C = \frac{A-B}{A+B} \times 100$$

and

$$\delta c = \frac{1}{\sqrt{A+B}} \times 100$$

Where A = observed rate of uptake (cpm) in the right tibia (inoculated)

B = observed rate of uptake (cpm) in the left tibia (control)

C = % difference divided by the sum of the observed count rates

δc = % error expected in C

Tables 11-17 present the data of 7 rabbits studied according to this protocol. Column 1 represents radiographic evaluation results, column 2 represents scintigraphic evaluations, column 3 presents the observed uptake rate of the tibiae in counts per minute, column 4 presents the difference in uptake between the two tibiae, and column 5 presents the calculated statistical differences related to the sum of the observed count rates and expected error for each calculation. Standard deviation or range observed in uptake was very small. A + sign in columns 4 and 5 shows that uptake was greater in the right tibia than the left and conversely, a - sign indicates uptake was greater in the left tibia than the right bone. In the 7 animals studied (rabbit 5 died on day 3 of the experiment) only rabbits 1 and 4 developed osteomyelitis in one leg as diagnosed by both scintigraphic and radiographic methods. Rabbit 1 developed the disease process in its left leg and rabbit 4 in its right leg. A definite trend was seen in this series of animals in that the static uptake results showed good correlation with scintigraphic interpretations and rather poor correlation was seen between radiographic interpretations and the static uptake studies. Using this analytic approach a general trend was seen in rabbit 1 in which uptake was generally greater in the left tibia than in the right bone from day 9 to day 13 but the calculated difference was approximately 2.2 ± 0.1% or less. Rabbit 4 showed a consistent difference in uptake between the two tibiae with more uptake in the right bone as indicated by the consistent presence of the positive sign in columns 4 and 5 of Table 14. Column 5 (Table 14) shows that uptake in the right tibia of rabbit 4 is always greater than in the left bone during the course of the experiment but for the single exception on day

TABLE II

Static Uptake Study Results of Rabbit #1

Day	Radiograph: Left tibia (Control)	Radiograph: Right tibia (Inoculated)	Scintiscan: Left tibia (Control)	Scintiscan: Right tibia (Inoculated)	Observed counts per minute: Left tibia (Control)	Observed counts per minute: Right tibia (Inoculated)	Difference in count rate	% Difference***
Pre-inoculation	N	N	N	N	* (a) 148712	144660	- 4,052	- 1.4 ± 0.2
					** (b) 162801	166215	+ 3,414	+ 1.0 ± 0.2
1	A-T	A-T	N	N	* (a) 195170	191793	- 3,377	- 0.9 ± 0.2
					** (b) 186123	196139	+10,016	+ 2.6 ± 0.2
3	A-T	A-T	N	N	* (a) 158373	160411	+ 2,038	+ 0.6 ± 0.2
					** (b) 138292	135159	- 3,133	- 1.1 ± 0.2
5	A-T	A-T	A	A	* (a) 245139	254780	+ 9,641	+ 1.9 ± 0.1
					** (b) 226171	235091	+ 8,920	+ 1.9 ± 0.1
7	A-O	A-O	A	N	* (a) 216520	222164	+ 5,636	+ 1.3 ± 0.2
					** (b) 187170	189392	+ 2,222	+ 0.6 ± 0.2
9	A-O	A-O	A	N	* (a) 240085	236407	- 3,678	- 0.8 ± 0.1
					** (b) 218875	217749	- 1,126	- 0.3 ± 0.2
11	A-O	A-O	A	N	* (a) 333499	318894	-14,605	- 2.2 ± 0.1
					** (b) 293725	292642	+ 1,083	+ 0.2 ± 0.1
13	A-O	A-O	A	A	* (a) 255161	244102	-11,055	- 2.2 ± 0.1
					** (b) 231831	229096	- 2,735	- 0.6 ± 0.1

N = Normal
A = Abnormal O = Osteomyelitis T = Trauma

*a = 30 minutes (average of 3 observations)
**b = 60 minutes (average of 3 observations)

*** % Difference = $\frac{A - B \times 100}{A + B} \pm \frac{1 \times 100}{\sqrt{A + B}}$

TABLE 12

Static Uptake Study Results of Rabbit #2

Day	Radiograph: Left tibia (Control)	Radiograph: Right tibia (Inoculated)	Scintiscan: Left tibia (Control)	Scintiscan: Right tibia (Inoculated)	Observed counts per minute: Left tibia (Control)	Observed counts per minute: Right tibia (Inoculated)	Difference in count rate	% Difference***
Pre-inoculation	N	N	N	N	* (a) 296151	294188	- 1,963	- 0.3 ± 0.1
					** (b) 299980	308857	+ 8,877	+ 1.5 ± 0.1
2	N	A-O	N	N	* (a) 189108	193695	+ 4,587	+ 1.2 ± 0.2
					** (b) 147694	147813	+ 119	+ 0.0 ± 0.2
4	N	A-O	N	N	* (a) 299357	303102	+ 3,745	+ 0.6 ± 0.1
					** (b) 275876	291090	+15,214	+ 2.7 ± 0.1
6	A-T	A-O	N	N	* (a) 339459	362671	+23,212	+ 3.3 ± 0.1
					** (b) 323178	333169	+ 9,991	+ 1.5 ± 0.1
8	N	A-O	N	N	* (a) 330871	321747	- 9,124	- 1.4 ± 0.1
					** (b) 303727	300411	- 3,316	- 0.5 ± 0.1
10	N	A-O	N	N	* (a) 340366	337488	- 2,878	- 0.4 ± 0.1
					** (b) 319912	315881	- 4,031	- 0.6 ± 0.1
12	N	A-O	N	N	* (a) 323542	319404	- 4,138	- 0.6 ± 0.1
					** (b) 305724	299605	- 6,119	- 1.0 ± 0.1
14	A-T	A-T	N	N	* (a) 350089	353325	+ 3,236	+ 0.5 ± 0.1
					** (b) 338677	331086	- 7,591	- 1.1 ± 0.1

N = Normal

A = Abnormal O = Osteomyelitis T = Trauma

*** % Difference = $\frac{A - B \times 100}{A + B} \pm \frac{1 \times 100}{\sqrt{A + B}}$

* a = 30 minutes (average of 3 observations)

** b = 60 minutes (average of 3 observations)

TABLE 13

Static Uptake Study Results of Rabbit #3

Day	Radiograph: Left tibia (Control)	Radiograph: Right tibia (Inoculated)	Scintiscan: Left tibia (Control)	Scintiscan: Right tibia (Inoculated)	Observed counts per minute: Left tibia (Control)	Observed counts per minute: Right tibia (Inoculated)	Difference in count rate	% Difference***
Pre-inoculation	N	N	N	N	* (a) 169812	163955	- 5,857	- 1.8 ± 0.2
					** (b) 137280	138944	+ 1,664	+ 0.6 ± 0.2
1	N	N	N	N	* (a) 153604	156537	+ 2,933	+ 0.9 ± 0.2
					** (b) 139624	138039	- 1,585	- 0.6 ± 0.2
3	N	A-T	A	A	* (a) 115225	111893	- 3,332	- 1.5 ± 0.2
					** (b) 108469	115400	+ 6,931	+ 3.1 ± 0.2
5	A-O	A-O	A	N	* (a) 251682	240399	-11,283	- 2.3 ± 0.1
					** (b) 235472	217754	-17,718	- 3.9 ± 0.1
7	A-O	A-O	A	N	* (a) 225614	193817	-31,797	- 7.6 ± 0.2
					** (b) 190056	182181	- 7,875	- 2.1 ± 0.2
9	A-O	A-O	N	N	* (a) 276779	273897	- 2,882	- 0.5 ± 0.2
					** (b) 248792	262840	+14,048	+ 2.7 ± 0.1
11	A-O	A-O	N	N	* (a) 297494	283294	-14,200	- 2.4 ± 0.1
					** (b) 258574	253074	- 5,500	- 1.1 ± 0.1
13	A-O	A-T	N	N	* (a) 286025	296295	+10,270	+ 1.8 ± 0.1
					** (a) 274523	279376	+ 4,853	+ 0.9 ± 0.1
15	A-O	A-O	N	N	* (a) 280414	269689	-10,725	- 1.9 ± 0.1
					** (b) 253884	247361	- 6,523	- 1.3 ± 0.1

N = Normal

A = Abnormal O = Osteomyelitis T = Trauma

*** % Difference = $\frac{A - B \times 100}{A + B} \pm \frac{1 \times 100}{\sqrt{A + B}}$

* a = 30 minutes (average of 3 observations)

** b = 60 minutes (average of 3 observations)

TABLE 14

Static Uptake Study Results of Rabbit #4

Day	Radiograph: Left tibia (Control)	Radiograph: Right tibia (Inoculated)	Scintiscan: Left tibia (Control)	Scintiscan: Right tibia (Inoculated)	Observed counts per minute: Left tibia (Control)	Observed counts per minute: Right tibia (Inoculated)	Difference in count rate	% Difference***
Pre-inoculation	N	N	N	N	* (a) 159071	163788	+ 4,717	+ 1.5 ± 0.2
					** (b) 118999	131019	+12,020	+ 4.8 ± 0.2
2	A-T	A-T	N	N	* (a) 106151	124303	+18,152	+ 7.9 ± 0.2
					** (b) 106849	114015	+ 7,166	+ 3.2 ± 0.2
4	A-T	A-O	N	A	* (a) 233324	248561	+15,237	+ 3.2 ± 0.1
					** (b) 208027	239783	+31,756	+ 7.1 ± 0.1
6	A-O	A-O	N	A	* (a) 217700	260046	+42,346	+ 8.9 ± 0.1
					** (b) 208320	251512	+43,192	+ 9.4 ± 0.1
8	A-O	A-O	N	A	* (a) 309588	330573	+20,985	+ 3.3 ± 0.1
					** (b) 258687	318637	+59,950	+10.4 ± 0.1
10	A-O	A-O	N	A	* (a) 257521	295705	+38,184	+ 6.9 ± 0.1
					** (b) 231616	277646	+46,030	+ 9.0 ± 0.1
12	A-T	A-O	N	A	* (a) 226899	262998	+36,099	+ 7.4 ± 0.1
					** (b) 220098	260027	+39,939	+ 8.3 ± 0.1
14	A-T	A-O	N	A	* (a) 535435	590737	+55,302	+ 4.9 ± 0.1
					** (b) 427809	495904	+68,095	+ 7.4 ± 0.1

N = Normal

A = Abnormal O = Osteomyelitis T = Trauma

*** % Difference = $\frac{A - B \times 100}{A + B} \pm \frac{1 \times 100}{\sqrt{A + B}}$

* a = 30 minutes (average of 3 observations)

** b = 60 minutes (average of 3 observations)

TABLE 15

Static Uptake Study Results of Rabbit #6

Day	Radiograph		Scintiscan		Observed counts per minute		Difference in count rate	% Difference***
	Left tibia (Control)	Right tibia (Inoculated)	Left tibia (Control)	Right tibia (Inoculated)	Left tibia (Control)	Right tibia (Inoculated)		
Pre-inoculation	N	N	N	N	* (a) 306512	308338	+ 1,826	+ 0.3 ± 0.1
					** (b) 286347	280960	+ 5,387	+ 0.9 ± 0.1
2	A-T	A-T	N	N	* (a) 183632	177068	- 6,564	- 1.8 ± 0.2
					** (b) 178136	176245	- 1,891	- 0.5 ± 0.2
4	A-O	A-T	A	N	* (a) 298844	294867	- 3,977	- 0.7 ± 0.1
					** (b) 304647	298804	- 5,843	- 1.0 ± 0.1
6	A-O	A-T	N	N	* (a) 285106	274888	-10,218	- 1.8 ± 0.1
					** (b) 269154	264391	- 4,763	- 0.9 ± 0.1
8	A-O	A-O	N	N	* (a) 359856	368648	+ 8,792	+ 1.2 ± 0.1
					** (b) 349790	322647	-27,143	- 4.0 ± 0.1
10	A-O	A-O	N	N	* (a) 303829	256840	-46,989	- 8.4 ± 0.1
					** (b) 308257	259131	-49,126	- 8.7 ± 0.1
12	A-O	A-O	N	N	* (a) 216398	211718	- 4,680	- 1.1 ± 0.2
					** (b) 199983	180223	-19,760	- 5.2 ± 0.2

N = Normal
A = Abnormal
O = Osteomyelitis
T = Trauma

*** % Difference = $\frac{A - B \times 100}{A + B} \pm \frac{1 \times 100}{\sqrt{A + B}}$

* a = 30 minutes (average of 3 observations)
** b = 60 minutes (average of 3 observations)

TABLE 16

Static Uptake Study Results of Rabbit #7

Day	Radiograph		Scintiscan		Observed counts per minute		Difference in count rate	% Difference***
	Left tibia (Control)	Right tibia (Inoculated)	Left tibia (Control)	Right tibia (Inoculated)	Left tibia (Control)	Right tibia (Inoculated)		
Pre-inoculation	N	N	N	N	* (a) 184005	173937	-10,068	- 2.8 ± 0.2
					** (b) 156853	153252	- 3,601	- 1.2 ± 0.2
1	A-T	N	N	N	* (a) 203094	208186	+ 5,092	+ 1.2 ± 0.2
					** (b) 171041	166802	- 4,239	- 1.3 ± 0.2
3	A-T	N	N	N	* (a) 248346	240833	- 7,513	- 1.5 ± 0.1
					** (b) 226175	215920	-10,155	- 2.3 ± 0.2
5	A-T	N	N	N	* (a) 216186	211927	- 4,259	- 1.0 ± 0.2
					** (b) 209130	196494	-12,636	- 3.1 ± 0.2
7	A-T	A-T	N	N	* (a) 190056	182181	- 7,875	- 2.1 ± 0.2
					** (b) 205959	178347	-27,612	- 7.2 ± 0.2
9	A-O	A-T	N	A	* (a) 279274	294778	+15,504	+ 2.7 ± 0.1
					** (b) 248788	262836	+14,048	+ 2.7 ± 0.1
11	A-T	A-T	N	N	* (a) 250636	228722	-21,914	- 4.6 ± 0.1
					** (b) 235263	220101	-15,162	- 3.3 ± 0.1
13	A-T	A-T	N	N	* (a) 203648	200085	- 3,563	- 0.9 ± 0.2
					** (b) 198371	200589	+ 2,218	+ 0.6 ± 0.2

N = Normal
A = Abnormal
O = Osteomyelitis
T = Trauma

*** % Difference = $\frac{A - B \times 100}{A + B} \pm \frac{1 \times 100}{\sqrt{A + B}}$

* a = 30 minutes (average of 3 observations)
** b = 60 minutes (average of 3 observations)

TABLE 17

Static Uptake Study Results of Rabbit #8

Day	Radiograph		Scintiscan		Observed counts per minute		Difference in count rate	% Difference***
	Left tibia (Control)	Right tibia (Inoculated)	Left tibia (Control)	Right tibia (Inoculated)	Left tibia (Control)	Right tibia (Inoculated)		
Pre-inoculation	N	N	N	N	* (a) 239840	250068	+10,228	+ 2.1 ± 0.1
					** (b) 227558	233441	+ 5,887	+ 1.3 ± 0.1
2	A-T	A-T	N	N	* (a) 130586	112970	-17,616	- 7.2 ± 0.2
					** (b) 134467	111211	-23,256	- 9.5 ± 0.2
4	A-O	A-O	N	N	* (a) 222430	233289	+10,859	+ 2.4 ± 0.1
					** (b) 205804	214384	+ 8,580	+ 2.0 ± 0.2
6	A-O	A-O	N	N	* (a) 210692	236824	+26,132	+ 5.8 ± 0.1
					** (b) 171924	226330	+54,406	+13.7 ± 0.2
8	A-O	A-O	N	N	* (a) 381789	368309	-13,480	- 1.8 ± 0.1
					** (b) 306329	281730	-24,599	- 4.2 ± 0.1
10	A-O	A-O	N	N	* (a) 232929	212680	-20,249	- 4.5 ± 0.1
					** (b) 209399	195725	-13,674	- 3.4 ± 0.2
12	A-O	A-O	N	N	* (a) 238610	213972	-24,638	- 5.4 ± 0.1
					** (b) 222199	217042	- 5,157	- 1.2 ± 0.2

N = Normal

A = Abnormal

O = Osteomyelitis

T = Trauma

*** % Difference = $\frac{A - B \times 100}{A + B} \pm \frac{1 \times 100}{\sqrt{A + B}}$

* a = 30 minutes (average of 3 observations)

** b = 60 minutes (average of 3 observations)

2, 60 minutes after injection of the radiotracer. These patterns were consistent and definite in that the observed trend was seen each time. Occasionally, differences in increased uptake were seen in column 5 in the other rabbits, e.g. rabbit 6 on days 8 and 10 and rabbit 8 on day 6, but these differences were not seen consistently day after day in that the direction of change and calculated difference did change from day to day. These calculated differences of uptake could have been due to increased uptake of radiotracer in normally "hot" areas of bone such as the epiphysis in young rabbits' bones which could not easily be seen by the physicians interpreting the scintiscans (Gu80). The radiographs were often interpreted as being abnormal while no differences could be seen in the scintiscans and no trends were observed in the static uptake data to support radiographic interpretation.

In brief summary, a positive trend could be observed between static uptake analysis and scintigraphic interpretation in that the direction of the sign was constant for a number of days if only one leg was affected, and that when using this analytical approach, observed differences in uptake between the tibiae appeared to be approximately 3% or greater. It must be noted here that if both legs were affected, uptake of bone-seeking radiopharmaceutical would increase in each tibia and these trends would not be evident.

G. Further Diagnostic Scintigraphic Evaluations of this Rabbit Model for Osteomyelitis.

This rabbit model for osteomyelitis was evaluated to be representative of the human disease process by histopathologic,

radiographic, and scintigraphic diagnostic procedures. To further evaluate this animal model, scintigraphically and radiographically osteomyelitis positive rabbits then underwent other diagnostic scintigraphic studies as described in the following sections.

1. ^{67}Ga Citrate Scintigram and Tissue Distribution Study

One mCi of ^{67}Ga citrate was injected intravenously into a rabbit with active osteomyelitis in its right tibia (as evaluated by radiographic and scintigraphic techniques) on day 41 after inoculation and gamma camera imaging was performed 24 hours later followed by a tissue distribution study done 48 hours after injection of the radiotracer.

Photographic plate 5 illustrates the radiograph of the osteomyelitis lesion in the right tibia while photographic plate 6 illustrates the Tc-99m MDP bone image and photographic plate 7 illustrates the gallium-67 citrate scintiscan. The arrows indicate the infected site. Incongruence between the ^{99m}Tc methylene diphosphonate bone scintigram (Plate 6) and ^{67}Ga citrate scintiphoto (Plate 7) was seen with somewhat more radiogallium visualized in the region of infection than the ^{99m}Tc phosphate scintiscan. This difference in the relative distribution pattern of the two bone-seeking radiotracers was observed and reported by Rosenthall et al. (Ro79). This incongruence is seen because although both radiopharmaceuticals are bone-seekers, radiogallium is also localized in soft tissue near sites of infection. Reports in the literature note that this observed localization is due to (1) direct uptake of the radiogallium by microorganisms (Sh80) and specifically Staphylococcus aureus (Me78), the bacteria used in these

Photographic plate 5. Radiograph of hind limbs of a rabbit displaying gross osteomyelytic lesions.

Photographic plate 6. Scintigram (Tc-99m-MDP) of hind limbs of a rabbit displaying gross osteomyelytic lesions. (Corresponding to Radiographic plate 5.)

Photographic plate 7: Scintigram (Ga-67-citrate) of hind limbs of a rabbit with advanced osteomyelytic lesions. (Corresponding to Radiograph plate 5 and Tc-99m-MDP Scintigram plate 6.)

experiments to inoculate the rabbits, (2) in vivo radiolabelling of leucocytes, (3) lactoferrin binding at the site of infection, and (4) siderophore-^{67}Ga complex formation (Ho80, Ho80a) at the site of infection.

The tissue concentration results appear in Table 18. These data indicate that at 48 hours after injection 1.8% of the injected dose was present in the blood and that the majority of the radiotracer in the blood was not cell-asscociated but was plasma bound (Lo81,Te81) (present in the supernatant of the whole blood sample centrifuged at 800 G for twenty minutes). The relatively high amount of radioactivity in the kidneys compared to the other tissues is consistent with a major pathway of gallium-67 citrate excretion. Relatively high levels of tracer were also noted in the bone, especially in the joint and diseased bone mineral. More radiogallium was in the pus than in the diseased bone marrow in accordance with reports in the literature of in vivo radiolabelling of leukocytes with ^{67}Ga citrate(By73,Bu74,Ge74). The mechanisms of localization of ^{67}Ga citrate in inflammatory lesions are not yet fully understood and may be influenced by many different factors as discussed in the literature review of this topic.

2. ^{18}F-Fluoride Uptake Study

After intravenous injection of 53 μ Ci of ^{18}F-fluoride, a rabbit with an osteomyelitis positive affected right tibiofibula complex (as evaluated by radiographic and scintigraphic interpretation) was imaged with a positron camera.. The positron scintiscan (Photographic plate 8) taken 2 hours after the F-18 injection shows relatively increased uptake of the radiotracer in the area of infection of the right tibiofibula

TABLE 18

Tissue Concentration of ^{67}Ga Citrate in an Osteomyelitis-Positive Rabbit*

Tissue	% Injected Dose (per g or ml)
Whole Blood	0.0124 /ml
Plasma	0.0207 /ml
Lymph nodes	0.0092 /g
Spleen	0.0404 /g
Adrenal gland	0.0024 /g
Kidney	0.0705 /g
Small intestine	0.0189 /g
Liver	0.0382 /g
Marrow (control leg)	0.0040 /g
Diseased bone marrow (no pus)	0.0293 /g
Diseased bone pus	0.0536 /g
Bone joint (control leg)	0.1976 /g
Cortical bone (control leg)	0.1139 /g
Cortical bone (diseased leg)	0.1311 /g
Peripheral skeletal muscle (control leg)	0.0026 /g
Muscle adjacent to bone (control leg)	0.0056 /g
Muscle adjacent to diseased bone	0.0038 /g
1.0 ml containing 3.1×10^7 RBC/ml and 6×10^5 WBC	0.00035 /ml
Total monocytes from 18 ml whole blood containing 1.8×10^7 cells (lymphocytes and monocytes).	0.00001 /ml

* 48 hours after intravenous injection of 1.0 mCi Ga-67 citrate

Photographic plate 8. Scintigram (F-18-fluoride) of hind limbs of a rabbit with osteomyelytic lesions.

complex. The region of infection appearing as a "hot" spot (increased radioisotope uptake) in the scintiphoto could be due to increased blood flow to the affected region (Wo74, Ch78). Visual inspection of the scintiscan of the animal's hind legs showed increased uptake by the tibia in the same region indicated in the radiograph (Photographic plate 9) and ^{99m}Tc MDP scintiscan (Photographic plate 10) used to diagnose the disease process. The arrows indicate the affected site. The rapid blood clearance and bone uptake of this radiotracer would appear to make it a good agent in the assessment of metabolic bone disorders compared to the ^{99m}Tc labelled phosphorous compounds commonly used now. Thus a F-18 bone scan combined with a ^{67}Ga-citrate scintiscan and radiolabelled leukocyte investigation along with collaborating radiographs would appear to be particularly useful in the diagnosis of osteomyelitis.

3. ^{99m}Tc Sulphur Colloid Labelled Granulocytes

Rabbit granulocytes were labelled with ^{99m}Tc sulphur colloid and reinjected into osteomyelitis positive animals as evaluated by radiographic and scintigraphic interpretation. Three hours after injection of the radiolabelled leukocytes, gamma camera scintigraphs indicated that these radiolabelled granulocytes localized in the region of the infected area, thus acting as an agent specific for the inflammatory process. This region of increased radiotracer corresponded to the site of the osteomyelytic lesion as indicated by x-ray and Tc-99m MDP scintigraphy, but with the Tc-99m labelled granulocytes study, a considerable amount of soft tissue uptake surrounding the affected bone was also seen. The radiolabelling procedure of granulocytes with Tc-99m sulphur colloid is relatively simple with minimal cell manipulation.

Photographic plate 9. Radiograph of hind limbs of a rabbit with osteomyelytic lesions. (Corresponding to F-18 Scintigram plate 8.)

Photographic plate 10. Scintigram (Tc-99m-MDP) of hind limbs of a rabbit with osteomyelytic lesions. (Corresponding to F-18 Scintigram plate 8 and Radiograph plate 9.)

Photon flux from the reinjected granulocytes was sufficient to provide scintigraphic images and the information provided was specific for inflammatory lesions as reported by other workers (Le76a, An75, Ba77).

4. Bone Marrow Uptake of ^{99m}Tc Sulphur Colloid

In the experimental procedure of the present study, bone marrow uptake scintigrams were obtained from two rabbits which demonstrated asymmetric uptake of ^{99m}Tc methylene diphosphonate consistent with that found in human osteomyelitis and with similarly abnormal radiographs. The marrow uptake scintiscan was made 3 hours after the intravenous injection of ^{99m}Tc sulphur colloid to ensure localization of the radiopharmaceutical into the reticuloendothelial system. Several other studies have dealt with the localization of Tc-99m SC in bone marrow of experimental animals. Martindale et al. (Ma80a) reported rat tissue distribution studies of ^{99m}Tc sulphur colloid and stated that at one hour after injection 0.26 ± 0.13% was found in the blood and 0.61 ± 0.26% in the marrow. Greenberg et al. (Gr66) reported that 2.8% of the injected dose of Tc-99m SC was found within the bones of a dog sacrificed 24 hours after injection of the radiopharmaceutical.

The ^{99m}Tc SC scintigrams obtained from one of the infected animals (Photographic plates 11 and 12) on days 26 and 36 after inoculation indicated that the disease process destroyed some of the reticuloendothelial portion of the bone marrow. The arrows in Photographic plates 11 and 12 indicate the affected site. It is imperative that at least 2 such scintiscans using the same radiotracer be obtained at different times to prove that changes in patterns of radiotracer distribution have occurred because it has been shown that

Photographic plate 11. Scintigram (Tc-99m sulphur colloid) of hind limbs of a rabbit with osteomyelitic lesions 26 days after inoculation.

Photographic plate 12. Scintigram (Tc-99m sulphur colloid) of hind limbs of a rabbit 36 days after inoculation (compare with Photographic plate 11).

reticuloendothelial and erythyropoietic function are not always mapped in the same areas of bone marrow when uptake of radiocolloid or radioiron are compared (Ne70, Va67). Thus, care must be exercised when evaluating bone marrow scintiscans with different radiotracers. The animal data from the present experiments suggest that the local bone reticuloendothelial functions has decreased in the infected limbs of the rabbit as the disease progressed but no conclusions can be made about the erythropoietic function based only on the ^{99m}Tc sulphur colloid study. Data has been published indicating that the tibiofibula complex of the rabbit has low hemopoietic activity (Br61).

The experimental data here support those reported by Feigin et al. (Fe74) who demonstrated decreased uptake of ^{99m}Tc sulphur colloid in the region of osteomyelitis in rabbits as compared with the contralateral unaffected limb at least 4 days before similar radiographic differences were observed. These workers suggested that the bone marrow scan may be of some value in the early diagnosis of osteomyelitis.

V. SUMMARY AND CONCLUSIONS

A. The rabbit model for osteomyelitis as described in this thesis serves as a useful model for study of the disease process as evaluated by histopathological, radiological, and scintigraphic techniques.

B. If gross bone structural malformations - specifically destructive bone changes and periosteal new bone formation as well as soft tissue inflammation, is used as the criteria for evaluation, scintigraphic imaging techniques can detect signs of the disease process several days before radiographic signs become evident.

C. When roentgenographs of high quality are produced and subtle signs are used as the criteria for evaluation, radiographic techniques can detect signs of the disease as early and as often as scintigraphic imaging techniques. Using these criteria for evaluation the radiographic analysis provided a sensitivity of 0.89 and a specificity of 0.68 while the scintigraphic analysis demonstrated a sensitivity of 0.42 and a specificity of 0.95.

D. Kinetic uptake studies demonstrated more uptake of ^{99m}Tc methylene diphosphonate in the diseased bone compared to the contralateral normal bone. Such increased uptake of Tc-99m MDP was evident within the first 10 minutes of intravenous injection of the radiopharmaceutical.

E. Static uptake studies indicate that infected bone consistently demonstrates more uptake of ^{99m}Tc MDP than normal contralateral bone.

F. Other scintigraphic diagnostic procedures have also demonstrated that this rabbit model for osteomyelitis is representative of the human disease process in that patterns of uptake consistent with those reported in the literature for the human clinical study with ^{18}F - fluoride, ^{67}Ga citrate, ^{99m}Tc sulphur colloid bone marrow uptake, and ^{99m}Tc sulphur colloid leukocyte scintiscans have been shown.

VI. BIBLIOGRAPHY

Ac74 Ackerhalt, RE, Blau, M, Bakshi, S, and Sondel, JA: "A comparative study of three ^{99m}Tc-labeled phosphorous compounds and ^{18}F-fluoride for skeletal imaging". J. Nucl. Med. 15: 1153, 1974.

Ae68 Aegerter, E and Kirkpatrick, JA: "Orthopedic Diseases". WB Saunders Company, Philadelphia, Pennsylvania, 1968.

An75 Anderson, BR, English, D, Akalin, HE, and Henderson, W: "Inflammatory lesions localized with technetium Tc 99m-labeled leukocytes". Arch. Inter. Med. 135: 1067, 1975.

As80 Ash, Judith M and Gilday, DL; "The futility of bone scanning in neonatal osteomyelitis: Concise communication". J. Nucl. Med. 21: 417, 1980.

Ba48 Babaranty, L: "Les osteopathies atrophiques". J. Radio. Electrol. Med. Nucl. 29: 333, 1948.

Ba58 Bauer, GCH and Ray, RD: "Kinetics of strontium metabolism in man". J. Bone. Joint. Surg. [Am] 40: 171, 1958.

Ba59 Bauer, GCH and Wendenberg, B: "External counting of ^{47}Ca and ^{85}Sr in studies of localised lesions in man". J. Bone Joint Surg. [Br] 41: 558, 1959.

Ba77 Bardfeld, PA, Boley, SJ, Sammartano, R, and Bontemps, R: "Scintigraphic diagnosis of ischemic intestine with technetium-99m sulfur colloid-labeled leukocytes". Radiology 124: 439, 1977.

Ba80 Balsam, D, Goldfarb, CR, Stringer, B, and Farrugia, S: "Bone scintigraphy for neonatal osteomyelitis: Simulation by intravenous calcium". Radiology 135: 185, 1980.

Be81 Berkowitz, ID and Wenzel, W: "Normal technetium bone scans in patients with osteomyelitis". J. Nucl. Med. 22: 486, 1981.*

Bi79 Billinghurst, MW and Jette, D: "Colloidal particle-size determination by gel infiltration". J. Nucl. Med. 20: 133, 1979.

Bl71 Blahd, WH (editor): "Nuclear Medicine" 2nd Edition, McGraw-Hill, New York, New York, 1971 (p.454).

Bl76 Blair, RJ and McAfee, JG: "Radiological detection of skeletal metastases: Radiographs versus scans". Int. J. Radiat. Oncol. Biol. Phys. 1: 1201, 1976.

Br59 Branemark, P-I: "Vital microscopy of bone marrow in rabbit". Scand. J. Clin. Lab. Invest. [Suppl] 38: 5, 1959.

Br61 Branemark, P: "Experimental investigation of microcirculation in bone marrow". Angiology 12: 293, 1961.

Bu73 Burleson, RL, Johnson, MC, and Head, H: "Scintigraphic demonstration of experimental abscesses with intravenous ^{67}Ga citrate and ^{67}Ga labeled blood leukocytes". Ann. Surg. 178: 446, 1973.

Bu74 Burleson, RL, Johnson, MC, and Head, H: "*In vitro* and *in vivo* labeling of rabbit blood leukocytes with ^{67}Ga citrate". J. Nucl. Med. 15: 98, 1974.

Ca70 Capitanio, MA and Kirkpatrick, JA: "Early roentgen observations in acute osteomyelitis". Am. J. Roentgenol. 108: 488, 1970.

Ch64 Charkes, ND and Sklaroff, DM: "Early diagnosis of metastatic bone cancer by photoscanning with strontium-85". J. Nucl. Med. 5: 168, 1964.

Ch75 Charkes, ND, Philips, C, and Malmud, LS: "Bone tracer uptake: Evaluation by a new model". J. Nucl. Med. 16: 519, 1975.*

Ch78 Charkes, ND, Makler Jr, PT, and Philips, C: "Studies of skeletal tracer kinetics. I. Digital-computer solution of a five-compartment model of [^{18}F] fluoride kinetics in humans". J. Nucl. Med. 19: 1301, 1978.

Ch79 Charkes, ND, Brookes, M, and Makler Jr, PT: "Studies of skeletal tracer kinetics. II. Evaluation of a five-compartment model of [^{18}F] fluoride kinetics in rats". J. Nucl. Med. 20: 1150, 1979.

Co71 Costeas, A, Woodard, HQ, and Laughlin, JS: "Comparative kinetics of calcium and fluoride in rabbit bone". Radiat. Res. 46: 317, 1971.

Co74 Cox, PH: "^{99}Tc^{m} complexes for skeletal scintigraphy. Physico-chemical factors affecting bone and bone marrow uptake". Br. J. Radiol. 47: 845, 1974.

Cr75 Creutzig, H: "Bone imaging with F-18 and Tc-99m-EHDP after total hip replacement". J. Nucl. Med. 16: 522, 1975*

Da75 D'Ambrosia, RD, Riggins, RS, De Nardo, SJ, and De Nardo, GL: "Fluoride-18 scintigraphy in avascular necrotic disorders of bone". Clin. Orthop. 107: 146, 1975.

Da76 Davis, MA and Jones, AG: "Comparison of ^{99m}Tc-labeled phosphate and phosphonate agents for skeletal imaging". Semin. Nucl. Med. 6: 19, 1976.

De75 Deysine, M, Rafkin, H, Russell, R, Teicher, I, and Aufses, AH: "The detection of acute experimental osteomyelitis with ^{67}Ga citrate scannings". Surg. Gynecol. Obstet. 141: 40, 1975.

De76 Deysine, M. Rosario, E, and Isenberg, HD: "Acute hematogenous osteomyelitis: An experimental model". Surgery 79: 97, 1976.

Du73 Dunson, GL, Stevenson, JS, Cole, CM, Mellor, MK, and Hosain, F: "Preparation and comparison of Tc-99m diphosphonate, polyphosphate, and pyrophosphate nuclear bone imaging radio-pharmaceuticals". Drug. Intell. Clin. Pharm. 7: 470, 1973.

Du75 Duszynski, DO, Kuhn, JP, Alfshani, E, and Riddlesbeger, MM: "Early radionuclide diagnosis of acute osteomyelitis". Radiology 117: 337, 1975.

Dy79 Dye, SF, Lull, RJ, McAuley, RS, Van Dam, BE, and Young, W: "Time sequences of bone and gallium scan changes in acute osteomyelitis: An animal model". J. Nucl. Med. 20: 647, 1979.*

Eg79 Ege, GN and Warbick, A: "Lymphoscintigraphy: A comparison of ^{99}Tc^{m} antimony sulfide colloid and ^{99}Tc^{m} stannous phytate". Br. J. Radiol. 52: 124, 1979.

En75 English, D and Anderson, BR: "Labeling of phagocytes from human blood with ^{99m}Tc-sulfur colloid". J. Nucl. Med. 16: 5, 1975.

Fe74 Feigin, DS, Strauss, HW, and James, AE: "Detection of osteo-myelitis by bone marrow scanning". J. Nucl. Med. 15: 490, 1974.*

Fe77 Feigin, DS: Personal communciation. Armed Forces Institute of Pathology, Washington, District of Columbia, United States of America.

Fl61 Fleming, WH, McIlraith, JD, and King ER: "Photoscanning of bone lesions utilizing strontium 85". Radiology 77: 635, 1961.

Fr68 Francis, MD, Gray, JA, and Griebstein, WJ: "The formation and influence of surface phases on calcium phosphate solids". Adv. Oral. Biol. 3: 83, 1968.

Fr78 Freeman, LM and Blaufox, MD (editors): Semin. Nucl. Med. 8: No. 3, 1978.

Fr79 Francis, MD, Tote, AJ, Bendict, JJ, and Bevan, JA: "Radiopharmaceuticals II. Proceedings. 2nd International symposium on radiopharmaceuticals, March 19-22, 1979." Seattle, Washington, 1980.

Ga69 Gardner, E, Gray, DJ, and O'Rahilly, R (editors): "Anatomy", WB Saunders Company, Toronto, Ontario, 1969.

Ga75 Garnett, ES, Bowen, BM, Coates, G, and Nahmias, C: "An analysis of factors which influence the local accumulation of bone-seeking radiopharmaceuticals". Invest. Radiol. 10: 564, 1975.

Ga77 Garnett, ES, Cockshott, WP, and Jacobs, J: "Classical acute osteomyelitis with a negative bone scan". Br. J. Radiol. 50: 757, 1977.

Ge74 Gelrud, LG, Arsenault, JC, Milder, MS, Kramer, RJ, Swann, SJ, Canellos, GP, Johnston, GS: "The kinetics of ^{67}gallium incorporation into inflammatory lesions: experimental and clinical studies". J. Lab. Clin. Med. 83: 489, 1974.

Ge74a Genant, HK, Bautovich, GJ, Singh, M. Lathrop, KA, and Harper, PV: "Bone-seeking radionuclides: An in vivo study of factors affecting skeletal uptake". Radiology 113: 373, 1974.

Ge77 Gelfand, MJ and Silberstein, EB: "Radionuclide imaging: Use in diagnosis of osteomyelitis in children". J.A.M.A. 273: 245, 1977.

Gi75 Gilday, DL, Paul, DJ, and Paterson, J: "Diagnosis of osteomyelitis in children by combined blood pool and bone imaging". Radiology 117: 331, 1975.

Gi80 Gilday, DL: "Problems in the scintigraphic detection of osteomyelitis". Radiology 135: 791, 1980.

Gr66 Greenberg, ML, Atkins, HL, and Schiffer, LM: "Erythropoietic and reticuloendothelial function in bone marrow in dogs". Science 152: 526, 1966.

Gu80 Guillemart, A, Le Pape, A, Galy, G, and Besnard J-C: "Bone kinetics of calcium-45 and pyrophosphate labeled with technetium-96: An autoradiographic evaluation". J. Nucl. Med. 21: 466, 1980.

Ha34 Haldeman, KO: "Acute osteomyelitis. A clinical and experimental study". Surg. Gynecol. Obstet. 59: 25, 1934.

Ha76 Handmaker, H and Leonards, R: "The bone scan in inflammatory osseous disease". Semin. Nucl. Med. 6: 95, 1976.

Ha76a Handmaker, H and Giammona, ST: "The "hot joint" - increased diagnostic accuracy using combined ^{99m}Tc-phosphate and ^{67}Ga citrate imaging in pediatrics". J. Nucl. Med. 17: 554, 1976.

Ha77 Hamilton, RG, Alderson, PO, and McIntyre, PA: "Technetium-99m phytate as a bone-marrow imaging agent: Biodistribution studies in animals: Concise communication". J. Nucl. Med. 18: 563, 1977.

Ha78 Hayes, RL: "The medical use of gallium radionuclides: A brief history with some new comments". Semin. Nucl. Med. 8: 183, 1978.

Ha79 Hamilton, S and Hurley, GD: "Radio-isotope bone scanning in suspected osteomyelitis in children". Eur. J. Nucl. Med. 4: 325, 1979.

Ha80 Handmaker, H: "Acute hematogenous osteomyelitis: Has the bone scan betrayed us?". Radiology 135: 787, 1980.

He69 Hebb, DO and Favreau, O: "The mechanism of perception". Radiol. Clin. North Am. 7: 393, 1969.

He81 Henkin, RE, Woodruff, A, Chang, W, and Green, AM: "The effects of radiopharmaceutical incubation time on bone scan quality". J. Nucl. Med. 22: 486, 1981.*

Ho80 Hoffer, P: "Gallium and infection." J. Nucl. Med. 21: 484, 1980.

Ho80a Hoffer, P: "Gallium: Mechanisms". J. Nucl. Med. 21: 282, 1980.

Hu78 Hughes, S, Davies, R, Khan, R, and Kelly, P: "Fluid space in bone". Clin. Orthop. 134: 332, 1978.

Ja77 Jackson, FI, Schmidt, R, Shysh, A, and Lentle, BC: "The comparative sensitivity of bone scan and skeletal radiography in the detection of osteomyelitis". Ann. Roy. Coll. Phys. Surg. Canada 10: 84, 1977.

Jo76 Jones, AG, Francis, MD, and Davis, MA: "Bone scanning: Radionuclide reaction mechanisms". Semin. Nucl. Med. 6: 3, 1976.

Ka75 Kaye, M, Silverton, S, and Rosenthall, L: "Technetium-99m-pyrophosphate: Studies in vivo and in vitro". J. Nucl. Med. 16: 40, 1975.

Ki76 King, MA, Kilpper, RW, and Weber, DA: "A model of local accumulation of bone seeking radiopharmaceuticals". J. Nucl. Med. 17: 549, 1976.*

Ki77 King, MA, Kilpper, RW, and Weber, DA: "A model for accumulation of bone imaging radiopharmaceuticals". J. Nucl. Med. 18: 1106, 1977.

Kr74 Krishnamurthy, GT, Thomas, PB, Tubis, M, Endow, JS, Pritchard, JH, and Blahd, WH: "Comparison of ^{99m}Tc-polyphosphate and ^{18}F. 1. Kinetics." J. Nucl. Med. 15: 832, 1974.

Kr76 Krogsgaard, OW: "Technetium-99m sulfur colloid. In vitro studies of various commercial kits". Eur. J. Nucl. Med. 1: 31, 1976.

Ku75 Kundel, HL and Nodine, CF: "Interpreting chest radiographs without visual search". Radiology 116: 527, 1975.

Ku79 Kundel, HL: "Images, image quality and observer performance". Radiology 132: 265, 1979.

La79 Lavender, JP, Khan, RAA, and Hughes, SPF: "Blood flow and tracer uptake in normal and abnormal canine bone: Comparisons with Sr-85 microspheres, Kr-81m, and Tc-99m MDP". J. Nucl. Med. 20: 413, 1979.

Le76 Lentle, BC. Russell, AS, Percy, JS, Scott, JR, and Jackson, FI: "Bone scintiscanning updated". Ann. Intern. Med. 84: 297, 1976.

Le76a Lentle, BC, McPherson, TA, Scott, JR, and Jackson, FI: "Localization of acute inflammatory foci in man with ^{99m}Tc-S.C. labeled granulocytes". Clin. Nucl. Med. 1: 118, 1976.

Li77 Lisbona, R and Rosenthall, L: "Radionuclide imaging of septic joints and their differentiation from periarticular osteomyeltis and cellulitis in pediatrics". Clin. Nucl. Med. 2: 337, 1977.

Li79 Lim, TK, Bloomfield, VA and Krejcarek, G: "Size and charge distribution of radiocolloid particles". Int. J. Appl. Radiat. Isot. 30: 531, 1979.

Lo81 Logan, KJ, Ng, PK, Turner, CJ, Schmidt, RP, Terner, UK, Scott, JR, Lentle, BC, and Noujaim, AA: "Pharmacokinetics of radio-gallium in humans". Int. J. Nucl. Med. Biol. (In press).

Ma76 Majd, M and Frankel, RS: "Radionuclide imaging in skeletal inflammatory and ischemic disease in children". Am. J. Roentgenol. 126: 832, 1976.

Ma80 Makler Jr, PT and Charkes, ND: "Studies of skeletal tracer kinetics. IV. Optimum time delay for Tc-99m (Sn) methylene diphosphonate bone imaging." J. Nucl. Med. 21: 641, 1980.

Ma80a Martindale, AA, Papadimitriou, JM, and Turner, JH: "Technetium-99m antimony colloid for bone-marrow imaging". J. Nucl. Med. 21: 1035, 1980.

Me75 Merrick, MV, Gordon-Smith, EC, Lavender, JP, and Szur, L: "A comparison of ^{111}In with ^{52}Fe and ^{99m}Tc-sulfur colloid for bone marrow scanning". J. Nucl. Med. 16: 66, 1975.

Me76 Metz, CE, Starr, SJ, and Lusted, LB: "Observer performance in detecting multiple radiographic signals". Radiology 121: 337, 1976.

Me78 Menon, S, Wagner, HN, and Tsan, M-F: "Studies on gallium accumulation in inflammatory lesions: II. Uptake by Staphylococcus aureus: Concise communication". J. Nucl. Med. 19: 44, 1978.

Mo59 Morgan, JD: "Blood supply of growing rabbit's tibia". J. Bone Joint Surg. [Br.] 41: 185, 1959.

Ne70 Nelp, WB, Gohil, MN, Larson, SM, and Bower, RE: "Long term effects of local irradiation of the marrow on erythron and RE cell function". Blood 36: 617, 1970.

Ni69 Nickerson, DS, Kazmierowsky, JA, Dossett, JH, Williams Jr, RC, and Quie, PG: "Studies of immune and normal opsonins during experimental Staphylococcal infection in rabbits". J. Immunol. 102: 1235, 1969.

No70 Norden, CW: "Experimental osteomyelitis. I. A description of the model". J. Infect. Dis. 122: 410, 1970.

No81 Norris, SH and Watt, I: "Radionuclide uptake during the evolution of experimental acute osteomyelitis". Br. J. Radiol. 54: 207, 1981.

Po70 Portman, GA: "Current Concepts in the Pharmaceutical Sciences: Biopharmaceutics". Lea & Febiger, Philadelphia, Pennsylvania, 1970. Chapter 1.

Ra74 Rafkin, H, Deysine, M. Teicher, I, Russell, R, and Aufses, Jr, A: "Detection of experimental osteomyelitis with gallium-67 citrate". Surg. Forum. 25: 485, 1974.

Ri74 Riggins, RS, De Nardo, GL, D'Ambrosia, R, and Goldman, M: "Assessment of circulation in the femoral head by ^{18}F scintigraphy". J. Nucl. Med. 15: 183, 1974.

Ri77 Rinsky, L, Goris, ML, Schurman, DJ, and Nagel, DA: "^{99}Technetium bone scanning in experimental osteomyelitis". Clin. Orthop. 128: 361, 1977.

Ro73 Rodet, A: "The classic: An experimental study on infectious osteomyelitis". Clin. Orthop. 96: 3, 1973.

Ro76 Rosenthall, L and Kay, M: "Observations on the mechanism of ^{99m}Tc-labeled phosphate complex uptake in metabolic bone disease". Semin. Nucl. Med. 6: 59, 1976.

Ro78 Rohlin, M, Larsson, A, Hammarstrom , L: "In vitro interaction between ^{99}Tc-m-labeled pyrophoshpate, ^{32}P-labeled pyrophosphate and rat tissues". Eur. J. Nucl. Med. 3: 249, 1978.

Ro79 Rosenthall, L, Lisbona, R, Hernandez, M, and Hadjippaulou, A: "^{99m}Tc-PP and ^{67}Ga imaging following insertion of orthopedic devices". Radiology 133: 717, 1979.

Ru76 Russin, LD and Straub, EV: "Unusual bone-scan findings in acute osteomyelitis. Case report". J. Nucl. Med. 17: 617, 1976.

Sa78 Saha, GB and Boyd, CM: "Plasma protein binding of ^{99m}Tc-pyrophosphate". Int. J. Nucl. Med. Biol. 5: 236, 1978.

Sa79 Saha, GB and Boyd, CM: "A study of protein-binding of ^{99m}Tc-methylene diphosphonate in plasma". Int. J. Nucl. Med. Biol. 6: 201, 1979.

Sc41 Scheman, L, Janota, M, and Lewin, P: "The production of experimental osteomyelitis". J.A.M.A. 117: 1525, 1941.

Sh80 Shysh, A, Mallet-Paret, S, Lentle, BC, Jackson, FI, McPherson, TA, and Johnson, GR: "Influence of intradermal BCG on the biodistribution of radiogallium in mice". Int. J. Nucl. Med. Biol. 7: 333, 1980.

Sh81 Shysh, A. Mallet-Paret, S, Lentle, BC, Jackson FI, McPherson, TA, and Johnson, GR: "Altered biodistribution of radiogallium following BCG treatment in mice". Int. J. Nucl. Med. Biol., 1981. (In press).

Si76 Siegel, BA, Donovan, RL, Alderson, PO, and Mack, GR: "Skeletal uptake of ^{99m}Tc-diphosphonate in relation to local blood flow". Radiology 120: 121, 1976.

Sn57 Snapper, S: "Bone disease in medical practice". Grune and Stratton, Inc., New York, New York, 1957.

Sq69 Squire, LF: "Perception related to learning radiology in medical school". Radiol. Clin. North Am. 7: 485, 1969.

St22 Starr, CL: "Acute hematogenous osteomyelitis". Arch. Surg. 4: 567, 1922.

St74 Steigman, J and Richards, P: "Chemistry of technetium 99m". Semin. Nucl. Med. 4: 269, 1974.

St75 Starr, SJ, Metz, CE, Lusted, LB, and Goodenough, DJ: "Visual detection and localization of radiographic images". Radiology 116: 533, 1975.

Su71 Subramanian, G and McAfee, JG: "A new complex of ^{99m}Tc for skeletal imaging". Radiology 99: 192, 1971.

Su72 Subramanian, G, McAfee, JG, Bell, EG, Blair, RJ, O'Mara, RE, and Ralston, PH: "^{99m}Tc-labeled polyphosphate as a skeletal imaging agent". Radiology 102: 701, 1972.

Su73 Subramanian, G, McAfee, JG, Mehter, A, Blair, RJ, and Thomas, FD: "^{99m}Tc stannous phytate: A new *in vivo* colloid for imaging the reticuloendothelial system". J. Nucl. Med. 14: 459, 1973.*

Su75 Subramanian, G, McAfee, JG, Blair, RJ, Kallfelz, FA, and Thomas, FD: "Technetium 99m-methylene diphosphonate - a superior agent for skeletal imaging: Comparison with other technetium complexes". J. Nucl. Med. 16: 744, 1975.

Su76 Subramanian, G, Rhodes, BA, Cooper, JF, and Sodd, VJ (editors): Radiopharmaceuticals". The Society of Nuclear Medicine, Incorporated, New York, New York, 1976. Chapter 34.

Su76a Subramanian, G. Rhodes, BA, Cooper, JF, and Sodd, VJ (editors): Radiopharmaceuticals". The Society of Nuclear Medicine, Incorporated, New York, New York, 1976 (p. 347).

Su76b Subramanian, G., Rhodes, BA, Cooper, JF, and Sodd, VJ (editors): "Radiopharmaceuticals". The Society of Nuclear Medicine, Incorporated, New York, New York, 1976 (p. 353).

Su80 Sullivan, DC, Rosenfield, NS, Ogden, J, and Gottschalk, A: "Problems in the scintigraphic detection of osteomyelitis in children". Radiology 135: 731, 1980.

Sw77 Swensson, RG, Hessel, SJ, and Herman, PG: "Omissions in radiology: Faulty search or stringent reporting criteria?" Radiology 123: 563, 1977.

Ta74 Takahashi, K: "Short half-lived radiocolloids for delineation of the reticuloendothelial system in the bone marrow". Sci. Rep. Res. Inst. Tohoku Univ.-C 21: 35, 1974.

Te81 Terner, UK, Noujaim, AA, Lentle, BC, Hill, JR and Wong, H: "Uptake of gallium complexes in canine sterile abscesses". Int. J. Nucl. Med. Biol. (In press).

Th38 Thompson, RHS and Dubos, RJ: "Production of experimental osteomyelitis in rabbits by intravenous injection of Staphylococcus aureus". J. Exp. Med. 68: 191, 1938.

Th69 Thomas, EL: "Search behavior". Radiol. Clin. North Am. 7: 403, 1969.

Va67 Van Dyke, D, Shkurkin, C, Price, D, Yano, Y, and Anger, HO: "Differences in distribution of erythropoietic and reticulo-endothelial marrow in hematologic disease". Blood 30: 364, 1967.

Wa68 Wagner Jr, Henry N (editor): "Principles of nuclear medicine". W.B. Saunders Company, Toronto, Ontario, 1968.

Wa70 Waldvogel, FA, Medoff, G, and Swartz, MN: "A review of clinical features, therapeutic considerations and ususual aspects. I.". N. Eng. J. Med. 282: 198, 1970.

Wa70a Waldvogel, FA, Medoff, G, and Swartz, MN: "A review of clinical features, therapeutic considerations and unusual aspects. II.". N. Engl. J. Med. 282: 260, 1970.

Wa70b Waldvogel, FA, Medoff, G, and Swartz, MN: "Osteomyelitis: A review of clinical features, therapeutic considerations and unusual aspects III.". N. Engl. J. Med. 282: 316, 1970.

Wa77 Warbick, A, Ege, GN, Henkelman, RM, Maier, G, and Lyster, DM: "An evaluation of radiocolloid sizing techniques". J. Nucl. Med. 18: 827, 1977.

Wa79 Warbeck-Creone, A: "Colloidal particle-size determinations by gel filtration". J. Nucl. Med. 20: 1098, 1979 (Letter to the editor).

We69 Weber, DA, Greenberg, EJ, Dimich, A, Kenny, PJ, Rotheschild, EO, Myers, WPL, and Laughlin, JS: "Kinetics of radionuclides used for bone studies". J. Nucl. Med. 10: 8, 1969.

Wi27 Wilensky, AO: "The mechanism and pathogenesis of acute osteomyelitis". Am. J. Surg. 3: 281, 1927.

Wo74 Wootton, R: "The single-passage extraction of ^{18}F in rabbit bone." Clin. Sci. 47: 73, 1974.

Wo75 Wootton, R: "^{18}F as an indicator for bone blood flow measurement". Br. J. Radiol. 48: 70, 1975.*

Ye69 Yerushalmy, J: "The statistical assessment of the variability in observer perception and description of roentgenographic pulmonary shadows". Radiol. Clin. North Am. 7: 381, 1969.

Zi52 Zilversmit, DB, Boyd, GA, and Brucer, M: "The effect of particle size on blood clearance and tissue distribution of radioactive gold colloids". J. Lab. Clin. Med. 40: 255, 1952.

* Abstracts

PUBLICATIONS

(1) Jackson, F. E., Schmidt, R., Shysh, A. and Lentle, B. C.: "The comparative sensitivity of bone scan and skeletal radiography in the detection of osteomyelitis". Ann. Roy. Coll. Phys. Surg. Canada 10: 84, 1977.

(2) Lentle, B. C., Schmidt, R. and Noujaim, A. A.: "Drug effects in radiotracer biodistribution". J. Nucl. Med. 19: 743, 1978.

(3) Logan, K. J., Ng, P. K., Turner, C. J., Schmidt, R. P., Terner, U. K., Scott, J. R., Lentle, B. C. and Noujaim, A. A.: "Comparative pharmacokinetics of ^{67}Ga and ^{59}Fe in humans". Int. J. Nucl. Med. Biol. (In press).

(4) Logan, K. J., Ng, P. K., Turner, C. J., Schmidt, R. P., Terner, U. K., Scott, J. R., Lentle, B. C. and Noujaim, A. A.: "Pharmacokinetics of radiogallium in humans". Int. J. Nucl. Med. Biol. (In press).